Targeting anti-apoptotic proteins with small dual binding ligands

Lina-Maria Nordvall

Lina-Maria Nordvall
Degree Thesis in Chemistry 45 ECTS
Master's Level
Report passed: 25 February 2014
Supervisor: Sofie Knutsson, Andreas Larsson, Luciana Auzzas

Cancermedicin som slår två flugor i en smäll önskas

Cancer är den tredje vanligaste dödsorsaken i världen och orsakar mycket lidande för såväl den drabbade med närstående som för samhället i stort. Detta kan vara i form av förlorad arbetskraft, sjukvårdskostnader samt kostnader som berör anhöriga. Därmed finns en strävan efter en mer effektiv men samtidigt patientvänlig behandling mot cancer. Prostatacancer drabbar i Sverige varje år ca 10 000 män och är den vanligaste typen av cancer i många i-länder. Antalet fall av prostatacancer har länge varit uppåtstigande och delvis beror det på ny effektivare typ av diagnostik, t. ex. PSA-provet. Men antalet som dör i prostatacancer har ändå varit stabilt och det beror delvis på förbättrad behandling.

Våra gener kodar för olika proteiner som vart och ett har sin speciella funktion i vår kropp. Ett av problemen med cancer är att ofta har flera gener förändrats, uttryckt lite annorlunda så är det flera saker som inte står rätt till i en och samma sjukdom. Det här kan innebära att många cancermediciner som bara riktar in sig på funktionen hos *ett* förändrat protein inte räcker till för att helt bromsa upp sjukdomsförloppet även om det också finns fördelar med sådana läkemedel, t. ex. eventuellt färre biverkningar. En annan behandling av cancer kan innebära att man kombinerar flera olika läkemedel för att komma åt flera olika problem. Många patienter tycker inte om en sådan behandling och dessutom kan man få nya biverkningar som uppkommer just pga en viss kombination av läkemedel.

Ett sätt att komma runt det här problemet skulle kunna vara att göra en viss substans som kan binda till och påverka funktionen hos flera proteiner och man skulle därmed komma åt flera problem med ett och samma läkemedel. Det är just vad vi ville göra i det här projektet. Det började med att man såg en likhet i utseendet hos två olika substanser som redan var kända för att rikta in sig på två olika proteiner som ofta är förändrade vid cancer. Proteinerna heter XIAP och IGF1R och båda hindrar cellerna i en tumör från att dö, fast det är just det de borde göra efter som de ställer till med sjukdom. Cancerceller är kända för att fortsätta leva och dela på sig fast de har sjukligt förändrade gener och borde dö för att gynna människan de bor i.

De två substanserna som liknade varandra (embelin och en nakijiquinonanalog) kunde bägge binda till båda proteinerna, men de var inte ideala som läkemedel. Med hjälp av beräkningar hittades liknande substanser som var mer lämpliga, men de var väldigt små och för att kunna se någon större effekt på cancerceller så gjorde vi dem lite större genom att addera kolkedjor. När substanserna var färdiga testades de på prostatacancerceller (PC-3 och 22Rv1) för att se om de kunde döda dem, och ja en av substanserna (5-F-2-hydroxy-3-propyl-bensoesyra) dödade 90 % av alla cellerna vid en koncentration av 400 µM. Men innan substansen kan inspirera till ny behandling måste man ta reda på hur cellerna dör och dessutom exponera friska prostataceller för samma substans eftersom den får bara döda cancerceller.

Abstract

Given that cancer is commonly associated with a multitude of aberrantly regulated proteins, as a result of multiple mutations, a cancer selective but multi-targeted approach to treat cancer is potentially beneficial. However, a multi-drug therapy might reduce patient compliance and lead to drug-drug side effects. By combining multiple but limited targets in the scope of one drug these problems could be reduced, and by starting from small molecules, more room is left for chemical optimization. Therefore, synthetic methods to modify dual binder fragments for the in cancer frequently overexpressed proteins XIAP and IGF1R were developed in an attempt to optimize their binding. The resulting compounds were then evaluated for their anti-proliferative effect on PC-3 and 22Rv1 prostate cancer cells. One of the synthesized molecules showed to be a promising lead and significantly decreased proliferation in both cell lines.

Abbreviations

Ac	Acetyl
Bad	Bcl-2-associated death promoter
Bn	Benzyl
d	Day
DMF	*N,N*-Dimethylformamide
Dppf	1,1′-Bis(diphenylphosphino)ferrocene
dPPP	1,3-Bis(diphenylphosphino)propane
DR	Death receptor
Et	Ethyl
h	Hour
HTS	High-Throughput Screening
Me	Methyl
min	Minute
ML-IAP	Melanoma inhibitor of apoptosis protein
MTT	3(4,5-dimethylthiazozyl-2)-2,5 diphenyl tetrazolium bromide
MWI	Microwave irradiation
NBS	N-Bromosuccinimide
NF- κB	Nuclear factor kappa-light-chain-enhancer of activated B cells
NMP	1-Methyl-2-pyrrolidinone
Ph	Phenyl
RIP1	Receptor interacting protein 1
rt	Room temperature
SPhos	2-Dicyclohexylphosphino-2′,6′-dimethoxybiphenyl
THF	Tetrahydrofuran
TLC	Thin layer chromatography
TRAIL	TNF-related apoptosis-inducing ligand
TTBP	Tri–tert–butylphosphine

Introduction

Cancer is one of the most common causes of death worldwide with only cardiovascular and infectious diseases harvesting more lives. Besides the suffering in affected families, the disease causes a tremendous cost for the society with the loss of work power, costs of medical treatment, and costs for dependents. The need for more efficient, but yet patient friendly anti-cancer treatments is therefore urgent. One of the most frequently diagnosed cancers in Western countries, North America, and Oceania is prostate cancer and its incidence is currently increasing, with better diagnostics being an important factor. However, advances in health care contribute to a steady level of mortality.[75]

Cancer is most often not caused by a single mutation, but rather a cluster of mutations acquired over years, wherein some are more critical than others. Indeed, for many malignancies therapies directed towards one target at a time do not work or works too slow. This enables cancer to get ahead of the treatment and eventually leads to the development of chemo resistance.[1] Due to its wide-ranging etiology, cancer should be treated in a multi-targeted manner to more efficiently eradicate the tumorous cells. However, the parallel use of a multitude of drugs increases the risk of poor patient compliance and tolerance. In addition to the adverse effects associated with each drug, drug-drug side effects are possible (i.e. the cocktail effect). By combining multiple targets in the scope of one ligand, we believe these problems can be reduced.

Many anticancer therapies today aims to induce apoptosis, but one of the hallmarks of cancerous cells are their inherent resistance to apoptosis.[2] Apoptosis, or programmed cell death, is a fundamental process involved in normal development and cell homeostasis, which with eyes for what is best for the organism and not for the individual cell provides protection against infectious agents as well as malignancies. The importance of apoptosis in normal physiology has evolved in extensive redundancy and crosstalk in its signaling pathways,[3] and a cancer cell often have multiple mutations involved in this death machinery, in order to escape it. This motivates the search for a multi-targeted anti-apoptotic drug.[4]

Key modulators in apoptosis are the highly conserved, cysteine-dependent aspartate-specific proteases (caspases) that activate each other in a cascade manner, and proteolytically cleave specific substrates in the cell, and thereby lead to the controlled break down of cell components during the cell death program.[5] Caspases can be divided into initiator- and effector caspases, where the initiator caspases activates pro-effector caspases and the effector caspases then do the actual cleavage of proteins associated with apoptosis.[6] The initiation of the cascade is negatively regulated by caspase inhibitors e.g. IAPs (inhibitor of apoptosis proteins).[7]

In addition to choosing target or targets for the ligand there are undoubtedly other problems to be dealt with during the development of new drugs, *e.g.* the size of the molecule. Large molecules tend to be non-specific hits in HTS, where they bind predominantly with hydrophobic interactions due to their size, and are no longer attractive leads when corrected for the molecular mass. This gives less room for optimization when aiming to keep good pharmacokinetic properties. Certainly, the screen is just as good as its contents and a good molecular library mitigates this problem. By starting from small and more

polar molecules with hydrogen bond donors and/or acceptors the chance of finding good lead compounds with more specific interactions is increased. In addition, this approach gives more room for chemical optimization, which anyhow tends to increase the molecules lipophilicity.[8]

In this study we aimed to make dual binders, and therefore found even more benefit from starting with small molecules, by increasing the chance that the molecule would fit into specific grooves of two different proteins, namely XIAP and IGF1R. Increased activity from these proteins is associated with establishment and progression of various types of cancer.[9, 10] In common, they have their ability to promote proliferation (*e.g.* via activation of NF-κB) and the ability to escape apoptosis through inactivation of pro-apoptotic factors like Bad and caspases.[9,10] IGF1R is crucial for the proliferation and survival of cancer cells with anchorage-independent growth[11] *i.e.* without contact with extracellular matrix, which makes the cells more likely to metastasize, and XIAP is one of the most potent inhibitor of apoptosis among the proteins in the IAP family.[12]

The idea of a dual binder stems from the structural similarity between the natural product and small-molecule XIAP inhibitor embelin[13] (**1**) and the nakijiquinone IGF1R inhibitor[14] (**2**) (Fig. 1). They both possess a quinone motif and this potentially toxic redox system make them poorly suited as drugs and the many ionizations states of the hydroxy quinone makes modeling difficult.

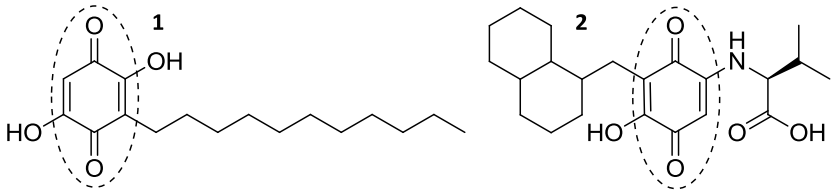

Figure 1. Embelin **1** and the nakijiquinone analogue **2** share the quinone motif.

Prior to this work, fragments with physicochemical properties resembling the dihydroxyquinone moiety of **1**, but without the redox system, were identified with the aid of a principal component analysis method. These fragments were then subjected to surface plasmon resonance for evaluation of their binding affinities towards the BIR3 domain of XIAP and the tyrosine kinase domain of IGF1R, respectively.

The aim of this project was to synthesize alkylated analogues to some of the fragments that showed (relatively) good binding to both of the proteins (Fig. 2) and then to evaluate them as pro-apoptotic agents in the human prostate cancer cell lines PC-3[15] and 22Rv1[16]. The introduction of an alkyl chain can increase the binding affinity to the proteins and better disclose the potential of the different fragments. We believe that restoration of the cancerous cells ability of undergoing apoptosis and the attenuation of proliferative signals, by inhibiting the potent anti-apoptotic and pro-proliferating proteins XIAP and IGF1R simultaneously, could give the patient a greater chance to combat cancer.

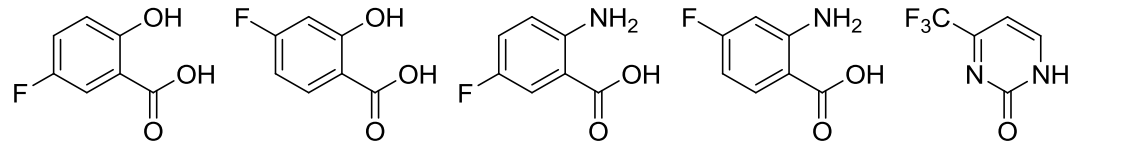

Figure 2. Dual binder fragments selected for alkylation.

Biological background

XIAP

Structure

The IAP family member XIAP (x-linked inhibitor of apoptosis protein) is an anti-apoptotic protein overexpressed in many types of cancer.[17] The protein consists of three N-terminal baculoviral IAP repeat domains (BIR1-3), a central UBA (ubiquitin-associated) domain and the C-terminal RING (really interesting new gene) domain.[9] The BIR domain, which characterizes all IAP members, was first discovered in baculovirus where it hindered the host cell (insect) from undergoing apoptosis upon infection.[18] The third BIR domain (BIR3) binds to and inhibits the initiator caspase 9, by sterically hindering its dimerization that is crucial for its activation. Another structurally important element is the linker region between BIR1 and BIR2 that inhibits the effector caspases 3 and 7 by binding to their active sites[19] (Fig. 3).

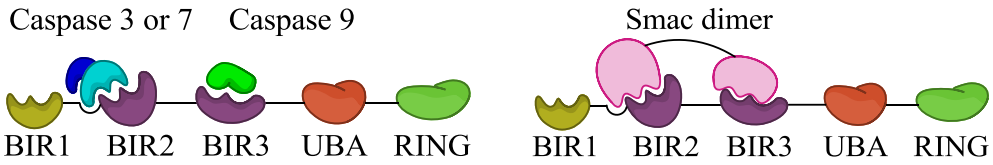

Figure 3. The tertiary structure of XIAP and its interaction with caspases and smac. By author.

Apoptosis

The course to apoptosis (Fig. 4) can be divided into an extrinsic and an intrinsic pathway, where the extrinsic way is activated from the cell membrane via the death receptor, and the intrinsic way is activated from the mitochondria in response to irradiation or other genotoxic stress. XIAP is unique in that it directly inhibits caspases involved in both pathways and acts quite downstream in the apoptosis signaling pathways, together this result in a substantial inhibition of apoptosis.[20] The death receptors are of different subtypes, but they are all members of the tumor necrosis factor receptor (TNFR) superfamily (*e.g.*TNF1R, Fas, and DR) and their respective ligands are members of the TNF superfamily (TNFα, Fas ligand, and TRAIL).[21] The different death receptors are associated with different adaptor proteins (Fig. 4) and vary in their capacity to induce apoptosis.

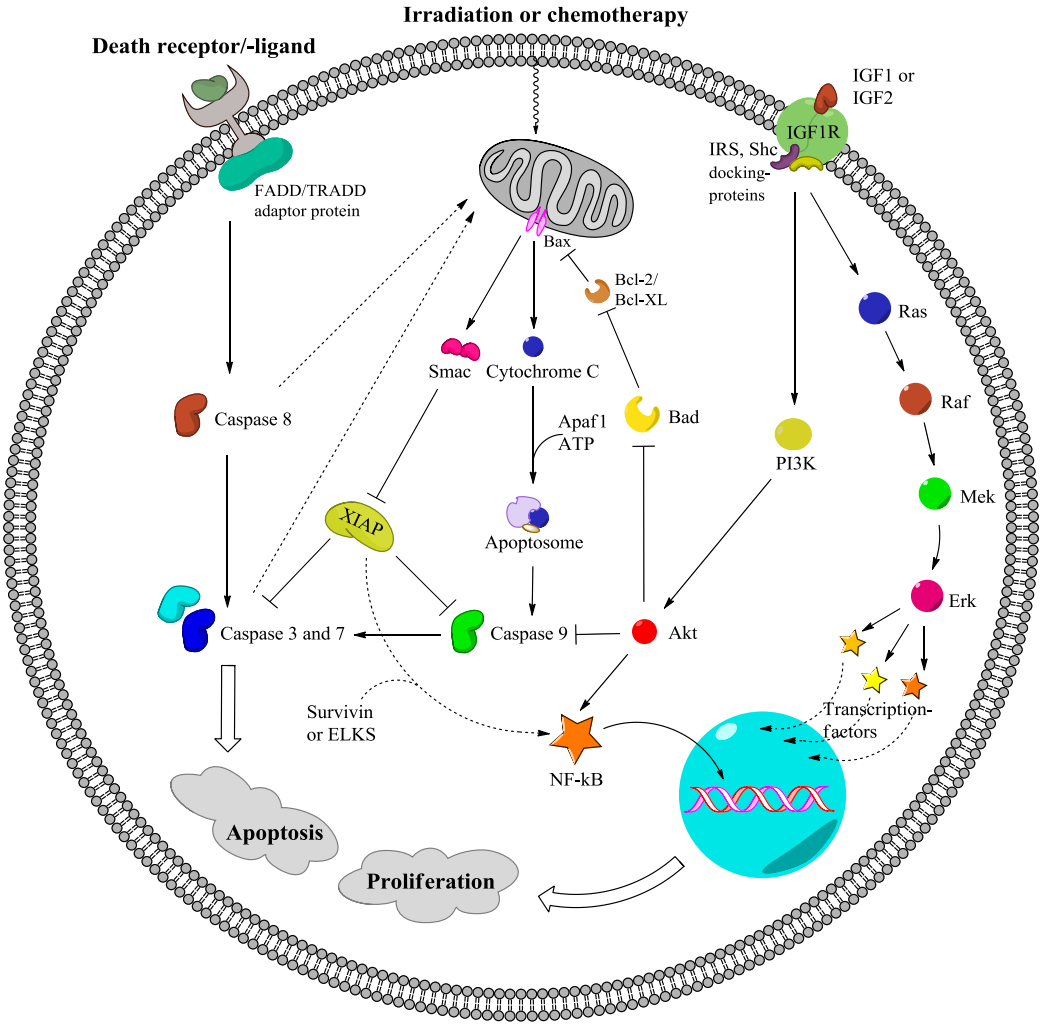

Figure 4. XIAPs and IGF1Rs role in apoptosis respective proliferation. By author.

Type 1 and type 2 cells

Cells can be divided into type 1 or type 2 depending on whether or not they need assistance from the mitochondria in order to achieve death receptor-induced (extrinsic) apoptosis. For type 1 cells (*e.g.* thymocytes), the activation of effector caspases 3 and 7 by initiator caspase 8 is sufficient to facilitate apoptosis, whereas in type 2 cells (*e.g.* hepatocytes) the mitochondria must assist with the release of pro-apoptotic factors in order to achieve a high enough concentration of activated effector caspases.[22] Two of the most important pro-apoptotic factors released from the mitochondria are cytochrome C and smac (second mitochondria-derived activator of caspases). Smac antagonizes the action of IAPs (e.g. XIAP) by blocking or binding to their caspase inhibitory sites and thereby relieve caspase inhibition, whereas cytochrome C forms a complex with Apaf-1 (apoptotic protease activating factor 1) and ATP (i.e. the apoptosome) that activates initiator caspase 9, which in turn activates effector caspase 3 and 7.[23] Caspase 3 (and -8) stimulates the release of pro-apoptotic factors by increasing the permeability of the outer mitochondrial membrane and XIAP can therefore cut this feed forward loop off by inhibiting caspase 3.[24]

Smac vs. small molecular inhibitors of XIAP

With a well conserved tetra peptide motif (AVPI), monomeric smac binds preferentially to the BIR3 caspase inhibitory site of XIAP and thus antagonize the inhibition of caspase 9. However, smac primarily exists as a dimer that binds to both BIR3 and BIR2. The BIR2 binding sterically blocks the linker region between BIR1 and BIR2 and therefore the inhibition of caspase 3 and 7 is also relieved (Fig. 3).[25] Many small-molecule inhibitors of XIAP mimics the AVPI binding motif and depending on how many IAP binding motifs is incorporated in the molecule they can be divided into mono- or bivalent i.e. binding one or two BIR domains.[9] Since these molecules are peptide mimetics they can be hampered with poor bioavailability due to their troublesome way into the cell, especially when administrated orally. Besides smac mimetic compounds there are also non-peptidic small-molecular inhibitors of XIAP[26] and antisense oligonucleotides (ASOs) that target the expression of XIAP[27]. The ASO strategy often needs continuous intravenous infusion (CIV) due to liver toxicity and poor oral bioavailability[27].

Bioavailability and ubiquitinations

The level of XIAP inside the cell is largely controlled by smac and the IAP family member survivin. Survivin stabilizes XIAP by binding to it and is overexpressed in most cancers.[28, 29] In addition, the survivin-XIAP complex activates NF-κB leading to increased proliferation and activation of cell-motility kinases, which in turn increases the tumors tendency of metastasizing.[30, 31]

Besides the BIR domains, XIAP is also characterized by its UBA domain that binds to ubiquitin in its various forms and the RING domain. The latter possess E3 ubiquitin ligase activity, which enables post translational modifications, for instance ubiquitinations of XIAP itself and its binding partners *e.g.* caspases, smac, and ELKS (glutamine, leucine, lysine, and serine-rich protein). These ubiquitinations tag some substrates for proteosomal degradation (*e.g.* smac and caspases) whereas ubiquitinated ELKS form a scaffold for signal-transduction and thereby enable XIAP to activate NF-κB mediated survival-signaling pathways.[31, 32]

IGF1R

Structure and interactions

The insulin-like growth factor 1 receptor (IGF1R) and its ligands IGF1, IGF2, and insulin comprises together with IGF2R and IR (insulin receptor) a signaling axis involved in normal growth and development, but also in the initiation and spreading of cancer. The bioavailability of IGFs is regulated by IGF binding proteins (IGFBPs) and the levels of IGFBPs are in turn regulated by IGFBP proteases.[33] The IGF1R is a tetrameric and membrane bound tyrosine kinase receptor composed of two identical extracellular and ligand binding α-subunits, and two identical β-subunits that spans the membrane to form a juxtamembrane domain and an intracellular tyrosine kinase domain.[34]

IGF signaling

The peptide hormones IGF1 and IGF2 are produced by the liver, by stromal fibroblasts, and by tumor cells[35] in response to growth hormone (GH), which the pituitary gland produces in response to GHRH (GH releasing hormone) from hypothalamus. Therefore, it is sometimes possible to treat cancer with GH- or GHRH antagonists, which are also used to treat gigantism.[36] Upon binding of IGF1 or IGF2 to the IGF1R the tyrosine kinase domain gets auto-phosphorylated and phosphorylates juxtamembrane

tyrosines, which enables binding of the docking proteins IRS (insulin receptor substrate 1) and SHC (Src homology 2 domain containing transforming protein 1). These proteins induce in parallel the Ras Raf Mek Erk (MAPK/ERK) - and PI3K/Akt signaling pathways.[37] The MAPK/ERK pathway promotes proliferation and cell cycle progression, in particular the G_1/S transition through activation of cyclinD_1.[38] The PI3K/Akt signaling activates Akt, which stimulates cell growth and inhibits apoptosis through inactivation of the pro-apoptotic proteins Bad and caspase 9 (Fig. 4).[39]

IGF2R as a counter actor of IGF1R signaling

Although IGF signaling is not unique in promoting cancerous proliferation it is essential for proliferation of cancer cells with anchorage-independent growth.[11] To balance the IGF signaling the IGF2R bind to and engulf IGF2 without any following MAPK/ERK or PI3K/Akt signal transduction, and thereby hinder it from activating IGF1R.[40] The gene encoding for IGF2R is considered as a tumor suppressor and in *e.g.* breast cancer, ovary cancer, melanoma, lymphoma and renal carcinoma the gene is frequently associated with loss of heterozygosity (LOH) meaning that each somatic cell only contains one copy of the *igf2r* allele and that an inactivating point-mutation of that copy, renders no functional gene left.[41]

IGF1R/IR heterodimers

Structurally, the IGF1R resembles the IR with 84 % sequence homology in the tyrosine kinase domain, but the ATP binding pocket is nearly identical.[42] The similarity between the IGF1R and the IR enables the receptors to heterodimerize i.e. form hybrid receptors of IGF1R/IR type, with one α-subunit and one β-subunit from each receptor.[43] In most cancer cells the majority of the IGF1 signaling occurs via the IGF1R receptor, but in some cancers signaling via the hybrid receptors is predominant.[44] Even more diversity comes from the two IR isoforms, i.e. IR_A and IR_B. All these possible combinations of dimers yields in receptors with different affinities for the ligands where the IGF1R binds strong to IGF1 and IGF2, but weak to insulin, the IGF1R/ IR_A binds strong to all three ligands, and the IGF1R/ IR_B binds strong to IGF1, weak to IGF2, and even weaker to insulin. The IR_A homodimers bind both insulin and IGF2, whilst IR_B homodimers only binds strongly to insulin. All these receptors except the last one are involved in proliferation and survival of normal and cancer cells.[45, 46]

The similarity between IGF1R and IR in the ATP binding pocket and the fact that most of the IGF1R tyrosine kinase inhibitors are designed to bind to this pocket makes it hard to find a selective IGF1R inhibitor. Consequently, the IR- and hybrid receptors are also affected. This can be an advantage since some cancers are driven by IGF1R/IR heterodimer signaling and since it is common with overexpression of IR on tumors and IR mediated resistance against IGF1R targeted therapy. However, it can also give unwanted side effects like hyperglycemia. Other strategies to diminish the IGF signaling include antisense RNA against IGF1R [47], monoclonal antibodies against IGF1R[48] or IGF[49], soluble IGF1R[50], and overexpression of IGF2R[51] or IGFBP1[52].

Results and discussion

The aim of this project was to alkylate selected XIAP and IGF1R dual binding fragments and in that way mimic the carbon chain of embelin and the decalin system in the nakijiquinone analogue (Fig. 1). The

synthesized compounds were thereafter evaluated for their anti-proliferative properties on PC-3 and 22Rv1 cells.

Alkylation of fluorinated salicylic acids

For the selected dual binding fragments (Fig. 2) we hypothesized that a Claisen rearrangement[53] of salicylic ethers could be used to obtain C-alkylated variants of those fragments (Fig. 5). This synthesis sequence also gives a possibility to compare the biological activities of the C-alkylated molecules with that of the ethers.

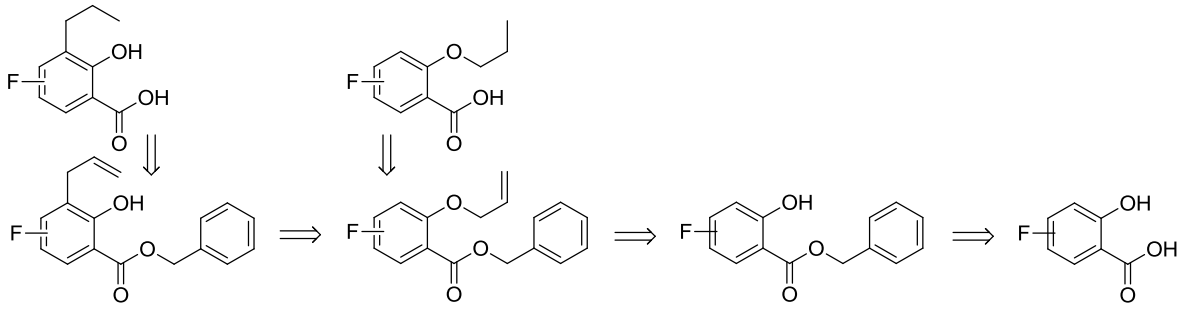

Figure 5. Retro synthetic analysis of alkylated fluoro-substituted salicylic acids.

To selectively allylate the phenol oxygen, the salicylic acids were first esterified with benzyl bromide and $KHCO_3$ in DMF according to published procedures for similar molecules (scheme 1 and 2).[54] The use of bicarbonate rather than K_2CO_3 has been reported to be a more selective method and indeed this alkylation shows good selectivity at room temperature. The protected salicylic acids were then allylated with allyl iodide and Cs_2CO_3 in DMF. In this case this method gave a higher yield (94 %) than the more classical procedure with refluxing acetone and K_2CO_3 (70 %), and cesium carbonate was used because of its good solubility in DMF.

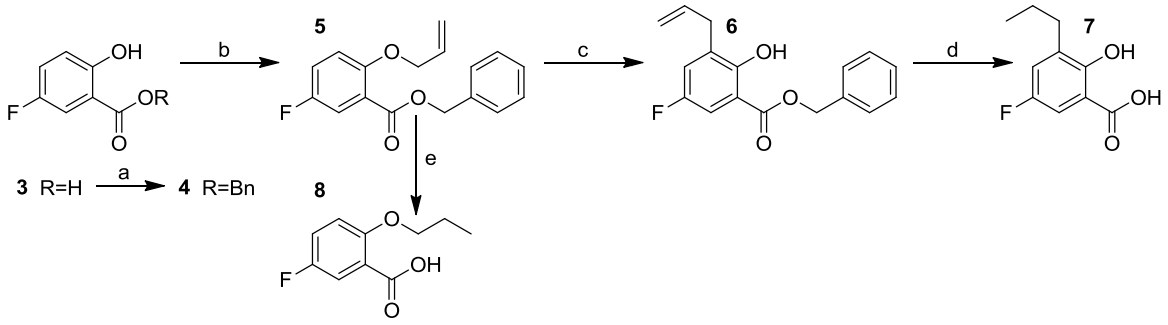

Scheme 1. Alkylation of 5-Fluoro-Salicylic acids. a) BnBr, $KHCO_3$, DMF, rt, 1 d, 91 %. b) Allyl iodide, Cs_2CO_3, DMF, rt, 2 d, 94 %. c) NMP, MWI 200°C, 6 h, 72 %. d) H_2, Pd/C, MeOH, rt, overnight, 98 %. e) H_2, Pd/C, MeOH, rt, 3 h, 94 %.

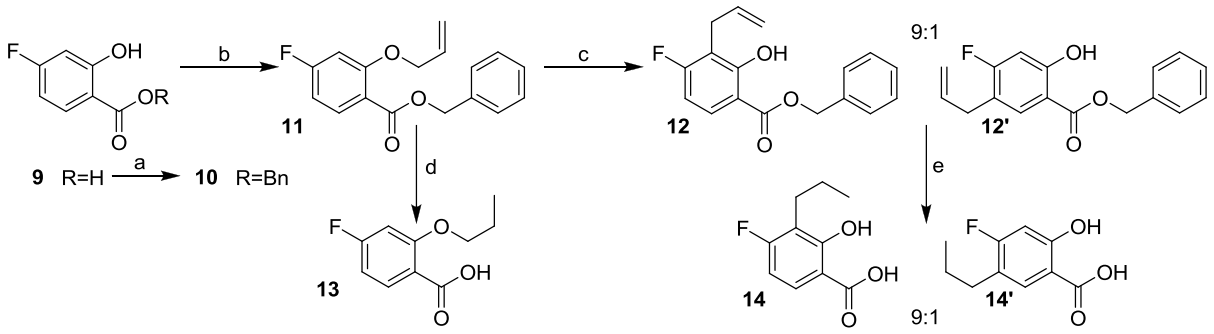

Scheme 2. Alkylation of 4-Fluoro-Salicylic acids. a) BnBr, $KHCO_3$, DMF, rt, 1 d, 90 %. b) Allyl iodide, Cs_2CO_3, DMF, rt, 2 d, 94 %. c) NMP, MWI 200°C, 8 h, 66 %. d) H_2, Pd/C, MeOH, rt, 3 h, 83 %.e) H_2, Pd/C, MeOH, rt, 3 h, 82 %.

The Claisen-rearrangement turned out to be more challenging, especially for the 4-fluoro salicylic acid **11** (Scheme 2), than the previous steps that worked smoothly. Generally the rearrangement required harsh conditions that tended to fragmentize the molecule by *e.g.* decarboxylation. Even so, it was possible to obtain the 5-fluoro rearranged molecule **6** (Scheme 1) in a satisfactory yield when running the reaction in microwave oven in NMP at 200°C for 6 hours.[55] These conditions were also applicable for the 4-fluoro substituted salicylic acid **11**, but here this reaction also yielded in the para-Claisen rearranged isomer **12'** that was inseparable from the product **12** in both flash column chromatography and LC-MS. Since the product could not be separated from the isomer, different conditions including various solvents such as xylenes, DMF, sulfolane, and H_2O at different temperatures and reaction times (200-250°C, 3-480 min), were applied to alter their proportions but either they changed in the wrong direction (favoring para-alkylation) or gave only traces of product. So the first reaction conditions tried turned out to be the best, yielding 9:1 of product and its isomer (**12** and **12´**, determined with H^1 NMR after purification).

To complete the synthesis of the four target compounds **7**, **8**, **13**, and **14**, the allyl ether and the rearranged molecules were hydrogenated with palladium on carbon, which conveniently saturated the alkyl chains and removed the benzyl ester. However, the 4-fluoro rearranged molecules (**14** and **14'**) were still inseparable.

Attempts were made to make the Claisen-rearrangement ortho selective *e.g.* by blocking the para-position with a bromine (Scheme 3). The bromination was accomplished with NBS in DMF and resulted in mono- and some di-brominated salicylic acids (**16** and **20**) that were separated with flash chromatography. Subsequent esterification and allylation of **16** gave entity **18** but this molecule did not give the rearranged product **19** using the developed conditions. One reason for this could be dehalogenation of the bromine, as suggested by the brown color of the crude reaction mixture. It is possible that the rearrangement could have been achieved at milder conditions but this was not investigated.

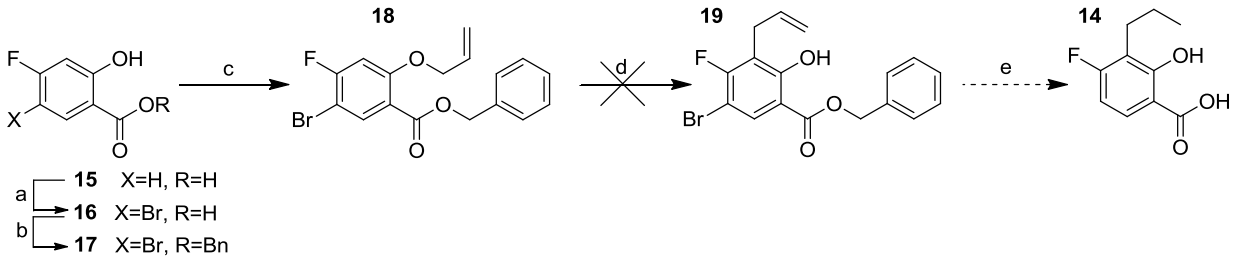

Scheme 3. Attempt to achieve ortho-selective rearrangement. a) NBS, DMF, rt, 1 d, 62 %. b) BnBr, $KHCO_3$, DMF, rt, 2 d, 98 %. c) Allyl iodide, Cs_2CO_3, DMF, rt, 2 d, 83 %. d) NMP, MWI 200°C, 6 h. e) H_2, Pd/C.

Since it is possible to selectively dehalogenate the bromine and reduce the allyl with hydrogen and Pd/C, another possible route of synthesis of ortho-alkylated entity **12** were investigated, where the dibrominated salicylic acid **20** was subjected to a ligand-free Suzuki coupling.[56] However, this reaction preferentially alkylated the para position to yield **21** (Scheme 4) and no ortho alkylated product was isolated. These Suzuki coupling conditions showed no dehalogenation and was also tried with the mono brominated entity **16** but resulted in a 1:1 mixture of product and starting material, which could not be separated with flash chromatography.

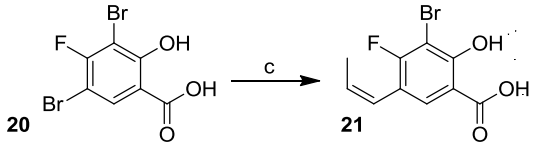

Scheme 4. Suzuki coupling. c) *cis*-Propenylboronic acid, $Pd(OAc)_2$, Na_2CO_3, H_2O, rt, 3 d, 24 %.

Alkylation of fluorinated anthranilic acids

The anthranilic acid fragments were proposed to be alkylated in a similar manner as the salicylic acids, but here it was possible to selectively allylate the amine before esterification (Fig. 6).

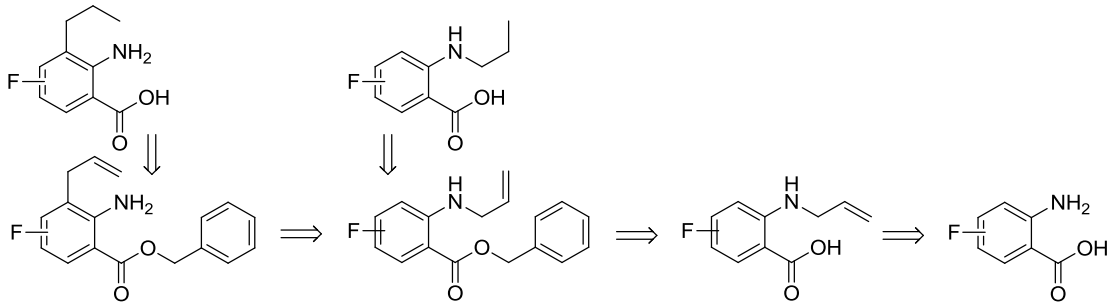

Figure 6. Retro synthetic analysis of alkylated fluoro-substituted anthranilic acids.

The 4-fluoro anthranilic acid **22** (Scheme 5) could be selectively *N*-mono allylated with allyl alcohol and tetrakis triphenylphosphine palladium in a two phase system with THF and water according to published procedures for similar molecules.[57] The molecule was thereafter esterified with the same method as described for the salicylic acids to yield **25**. Again the two first steps worked with convenience and the subsequent rearrangement was more troublesome. Anilines require more harsh conditions than the phenols for rearrangement to take place[58]. Therefore the Lewis acid $BF_3{\cdot}Et_2O$ was added to the reaction that this time was performed in sulfolane at 170°C in microwave oven for one hour,[59] but this could not give the product **26**. However, the allyl **23** could be hydrogenated to yield target molecule **24.**

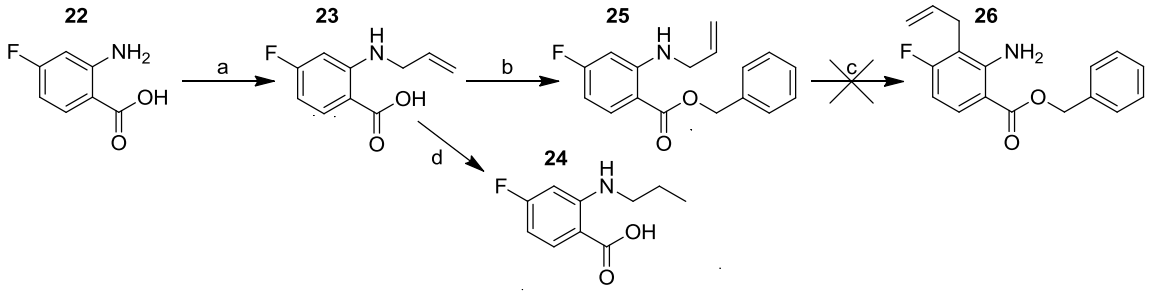

Scheme 5. Alkylation of 4-Fluoro-Anthranilic acid. a) Allyl alcohol, $Pd(PPh_3)_4$, THF/H_2O (1:1), rt, 3 d, 96 %. b) BnBr, $KHCO_3$, DMF, rt, 40 h, 93 %. c) $BF_3{\cdot}O(C_2H_5)_2$, sulfolane, MWI 170°C, 1 h. d) H_2, Pd/C, MeOH, rt, overnight, 54 %.

Selective *N*-mono allylation was also successfully performed on the 5-fluoro entity **27**, which thereafter could be hydrogenated to yield target molecule **30** (Scheme 6). The *N*-allyl molecule **28** was also subjected to rearrangement but without previous esterification (Scheme 6, step d). This reaction resulted in rearrangement of **28**, but yielded in a mixture of cis and trans propenylated (**29**) isomers, rather than the expected molecule **40**. The isomerized rearranged molecule **29** can potentially be used to achieve the hydrogenated C-propylated target molecule, but the purification was hampered by its zwitter ion properties and resulted in approximately 30 % yield with 80 % purity.

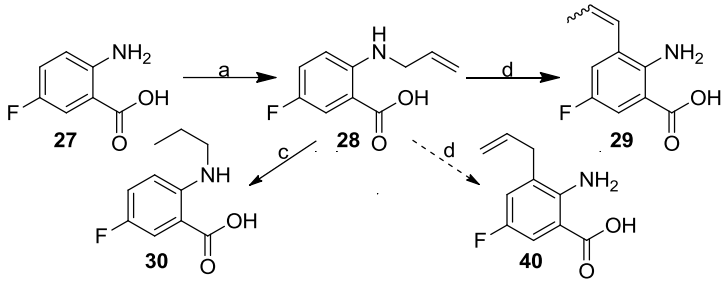

Scheme 6. Alkylation of 5-Fluoro-Anthranilic acid. a) Allyl alcohol, $Pd(PPh_3)_4$, THF/H_2O (1:1), rt, 3 d, 94 %. c) H_2, Pd/C, MeOH, rt, overnight, 57 %. d) $BF_3{\cdot}O(C_2H_5)_2$, sulfolane, MWI 170°C, 2 h.

Alkylation of CF_3-substituted pyrimidinone

The dual binding fragments (showed in Figure 2) also included a CF_3-substituted pyrimidinone fragment, and to accomplish the synthesis of the propylated pyrimidinone, a three step sequence involving Suzuki coupling was anticipated (Fig.7).

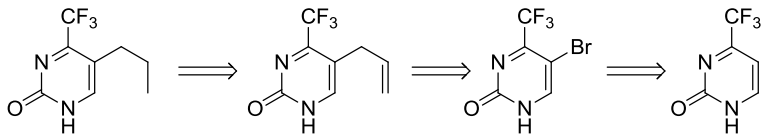

Figure 7. Retro synthetic analysis of propylated pyrimidinone

The pyrimidinone **31** was brominated according to published procedures[60] and yielded entity **32**. Subsequent attempts to synthesize **34** instead resulted in *N*-alkylated entity **33** (Scheme 7). This compound have previously been synthesized,[61] but in a different manner. As far as we know this kind of coupling, *i.e.* where the nucleophilic boronic acid couples to the nucleophilic carbamate nitrogen with simultaneous reduction of the brominated substrate, is not published before.

Anyhow, entity **33** was not the desired product and to get C-allylation many different conditions were tried out on entity **32** without success. Different solvents (dioxane:H_2O (9:1) and DMF:H_2O (9:1)), bases (KF, Na_2CO_3, and Cs_2CO_3), palladium sources ($Pd(OAc)_2$ and [Allyl Pd(II) $Cl]_2$), boronic acids/-esters (allylboronic acid pinacol ester and phenylboronic acid), ligands (dPPP, Herrmann's catalyst, $PdCl_2$ dppf, SPhos, and TTBP*HBF_4), temperatures (80-150°C), reaction times (10-60 min), and different proportions of equivalents of the reagents, were tested in various combinations.

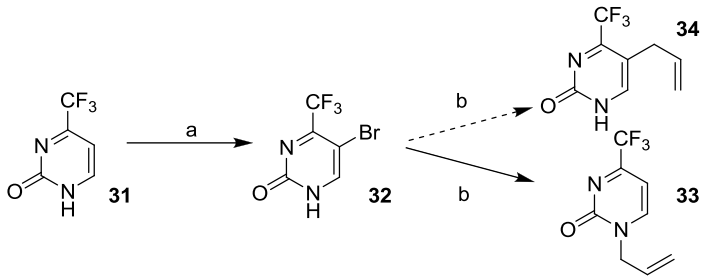

Scheme 7. Alkylation of CF_3-substituted pyrimidinone. a) Br_2, KOAc, HOAc, 80°C, 3 h, 87 %. b) Allylboronic acid pinacol ester, SPhos, $[PdCl(C_3H_5)]_2$, KF, Dioxane/H_2O (9:1), MWI, 110°C, 20 min, 33 %.

To protect the nitrogen position, entity **32** was benzylated to yield **35** and then subjected to the coupling reaction, but this gave only trace amounts of **36** (Scheme 8).

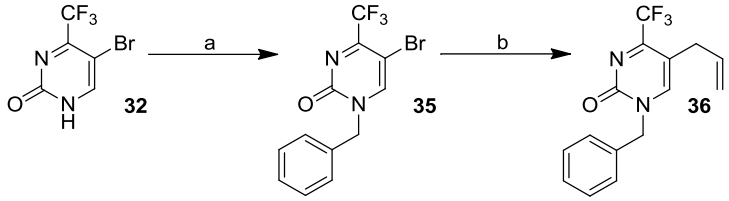

Scheme 8. Protection of the pyrimidinone nitrogen. a) BnBr, Cs_2CO_3, DMF, rt, 1 d, 26 %. b) Allylboronic acid pinacol ester, SPhos, $[PdCl(C_3H_5)]_2$, KF, Dioxane/H_2O (9:1), MWI, 110°C, 20 min, traces.

Another way to protect the nitrogen was investigated, where the chloro-substituted pyrimidine **37** was benzyloxylated with BnOH according to published procedures for similar molecules[62] to yield **38** (Scheme 9). Thereafter **38** was subjected to bromination, which unfortunately did not work despite longer reaction time and instead cleaved off the benzyl and lead back to molecule **32**, probably due to HBr formation.

After the end of this project, this molecule (**34**) could finally be synthesized by a coworker, by substitution of the chloride in **37** to the more electron-donating NH_2-group, subsequent bromination, and then subjecting the molecule to the Suzuki coupling.

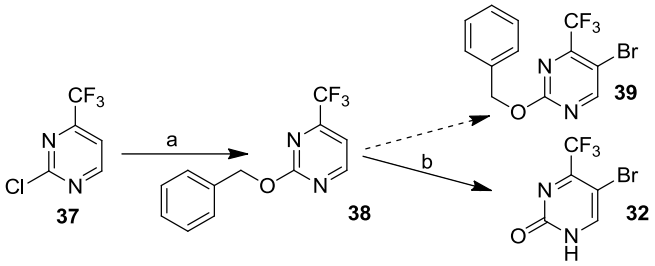

Scheme 9. Protection of the pyrimidine nitrogen. a) BnOH, CuI, 1.10-Phenanthroline, Cs_2CO_3, toluene, 120°C, 2 d, 65 %. b) Br_2, KOAc, HOAc, 80°C, 2 d.

Cell viability assay

Fragments that in surface plasmon resonance showed dual binding to the BIR3 domain of XIAP and to the tyrosine kinase domain of IGF1R were alkylated and then tested on PC-3 and 22Rv1 prostate cancer cells in MTT proliferation assay[63] to see if they were able to diminish the survival capacity of these cells. In metabolically active cells MTT is converted into purple formazan. The concentration of formazan can be measured with UV-spectrometry and is proportional to the amount of living cells.

The PC-3 cells are castration resistant whereas the 22Rv1 cells still are sensitive to androgen depletion.[15, 16] Depending on the tumors sensitivity towards androgens, the effect of tested inhibitors can differ completely, and therefore all tests were performed on these cell lines in parallel. The molecules that were tested are both the dual binder fragments and alkylated analogues of them (Fig. 8). In addition to the molecules which synthesis is described in this report also other molecules were tested.

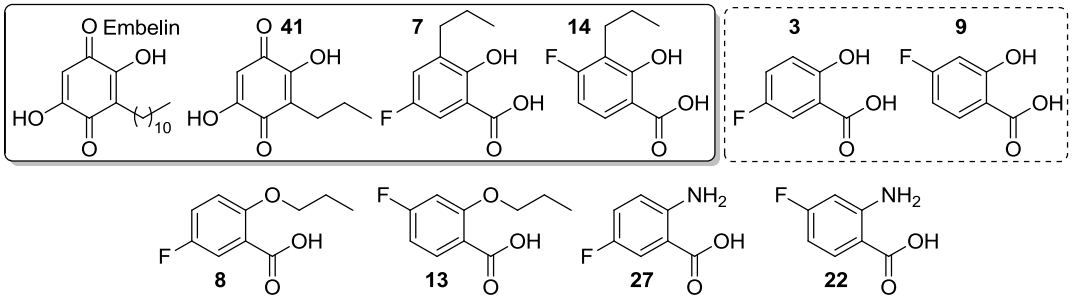

Figure 8. Molecules tested for their impact on viability in PC-3 and 22Rv1 cells. Molecules at the left top shows the greatest depletion of viability with values under 40 % compared to untreated control at 400 µM, molecules in the dashed box shows some effect on viability with values under 80 %, and the molecules on bottom shows the lowest or no effect on viability.

Initially, the known XIAP inhibitor embelin was tested as an anti-proliferative control. Embelin strongly reduces viability already at 20 µM in both cell lines, although the 22Rv1 cells seem to be more sensitive for this molecule (Fig. 9). Embelin downregulates the androgen receptor (AR) expression in androgen dependent LNCaP cells[64] and therefore it is possible that embelin like molecules have higher effect on androgen dependent prostate cancer cells, at least *in vivo*, compared to castration resistant cancer cells *e.g.* PC-3.

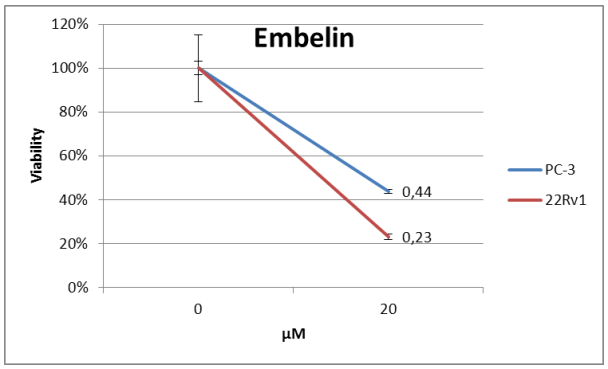

Figure 9. The XIAP inhibitor embelin significantly ($p<0.05$) reduces viability in PC-3 and 22Rv1 down to 44 % and 23 %, respectively compared to the untreated control at 20 µM. The values given are the avarages from four replicates, and the error bars shows the standard deviation within the replicates.

The prostate cancer cells 22Rv1 and PC-3 were then subjected to different concentrations of the synthesized molecules (except the alkylated anthranilic acids, due to lack of time) and then monitored for their proliferation (Fig. 10). The rearranged 4-fluoro salicylic acid (**14**) was tested as a 9:1 mixture together with its para-Claisen rearranged isomer, since they could not be separated. The synthesized molecules can by no means compete with the 11-carbon chained embelin for binding to XIAP and IGF1R and therefore the propyl analogue of embelin (**41**) was included in the test for comparison.

Out of 25 tested molecules (dual binding fragments and alkylated analogues) compound **7** is the most potent inhibitor of viability, besides embelin. The 22Rv1 cells are more sensitive to **7** than the PC-3 cells but the reduction of viability is strong in both cell lines. The other rearranged entity *i.e.* **14** which only differ in the position of its fluorine is less active than **7** but still one of the most active among all the tested molecules. Again, the 22Rv1 cell line was consequently more sensitive to **14** at 400 µM than PC-3 cells were when repeating the experiment three times. The ethers **13** and **8** shows no clear concentration dependent decrease in viability, whereas the propyl analogue of embelin (**41**) decreases viability in both cell lines from 200 µM but is less active than **7** and **14** in 22Rv1 cells.

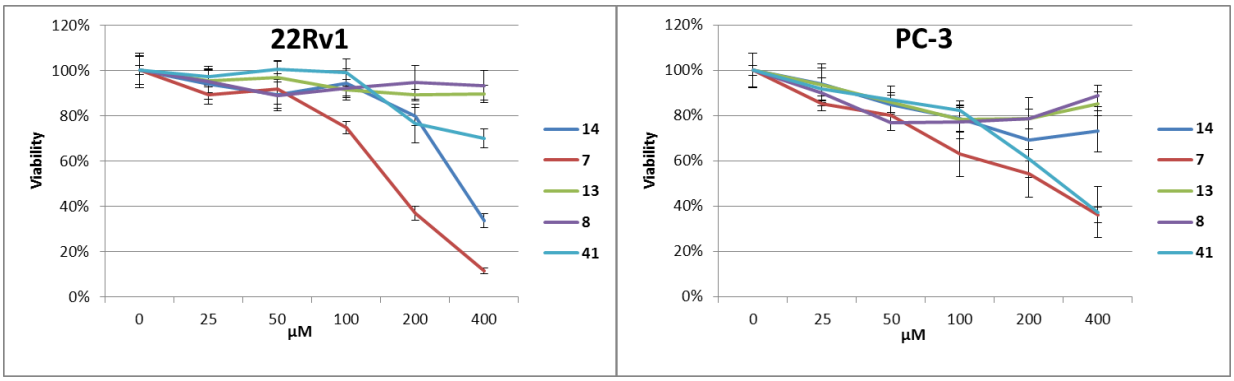

Figure 10. The rearranged 4-F-Salicylic acid (**14**) and 5-F-Salicylic acid (**7**) significantly ($p<0.05$) decreases viability in both cell lines from 200 and 100 µM, respectively compared to the untreated control, whereas the 4-F-Ether (**13**) and 5-F-Ether (**8**) shows no clear reduction of viability in either cell line. The propyl analogue of embelin (**41**) significantly decreases viability from 200 µM in both cell lines. The values given are the avarages from five replicates, and the error bars shows the standard deviation within the replicates.

The non-alkylated fragments showed no clear concentration dependent reduction in viability in either cell line although the salicylic acids have significant values around 70 % at 100 µM in the PC-3 cells the viability then increases again with increased concentration (Fig. 11). This is hard to explain, but the same pattern was observed with other molecules that can be expected to have solubility problems. The problem might on the other hand lay in the type of assay beeing used, since it is primarly the metabolic activity that is beeing measured and the viability is estimated indirectly. In turn, both decreased proliferation and/or increased apoptosis will reduce the viability and can not be distinguished in this assay. Particular molecules might influence the metabolic activity of the cells without actually increasing the number of cells.

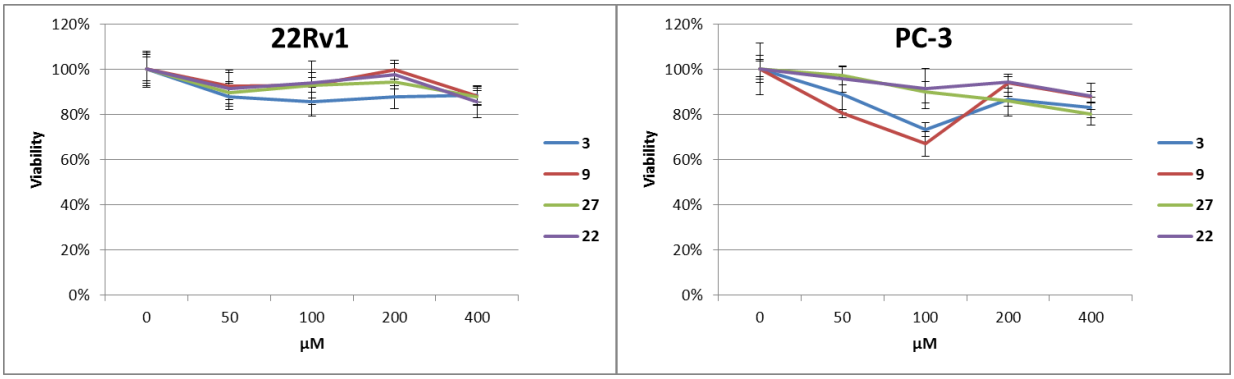

Figure 11. The dual binder fragments **3**, **9**, **27**, and **22** shows no clear concentration dependent reduction of viability compared to the untreated control in either cell line. The values given are the avarages from four replicates, and the error bars shows the standard deviation within the replicates.

The results indicate that we found an inhibitor of viability that is even more potent than the embelin analogue **41** but possess no toxic redox system. From the performed experiments, we cannot be certain that **7** actually reach the target proteins XIAP and IGF1R or even inside the cell rather than being generally toxic or interacting with other unexpected proteins. But due to its embelin and nakijiquinone resembling physiochemical properties, the likeliness that this molecule reaches XIAP and IGF1R is increased. Additional experiments including counting apoptotic vs. necrotic cells is needed to see that the cells do undergo apoptosis and detection of cleaved caspase 9 and 3 is needed to see that the apoptosis is of the caspase dependent variant. Also the selectivity of **7** towards cancer cells over normal cells should be compared. Embelin itself shows selectivity towards cancer cells with a IC_{50} value five-fold higher in normal PrECs compared to PC-3 cells (20 µM and 4 µM, respectively).[13]

Many prostate cancer cell lines, including PC-3 cells overexpress XIAP, whereas the levels of XIAP are very low in normal prostate epithelial cells (PrEC).[13] Still the selective intracellular activity of **7** on XIAP is not easily confirmed, since although the cells overexpress XIAP they are also characterized by plenty of other overexpressed proteins and potential binders. This bias can be mitigated if normal prostate epithelial cells are stably transfected with an extra copy or a high yielding mutant variant of the *xiap* gene and then compared with the untransfected normal PrECs upon treatment with **7**. The molecule is a potential XIAP inhibitor if the treatment with **7** can overcome the protective effects from overexpressed XIAP in the transfected cells upon apoptosis induction (with *e.g.* TRAIL, TNFα, Fas ligand or etoposide) compared to cells expressing low levels of XIAP(vector control).

The inhibition of IGF1R is hypothetically easier to confirm since there are both enzymatic kinase assays and specific antibodies available, which targets the tyrosine kinase domain in its phosphorylated form. The tyrosine kinase domain gets phosphorylated upon stimulation with *e.g.* recombinant IGF1, and if the synthesized molecule binds to and inhibits this domain there will be fewer antibodies bound compared to untreated cells stimulated with IGF1. This experiment was attempted, but unfortunately the utilized antibody was hampered with unspecific staining. It has been shown *in vitro* that IGF1R inhibition reduces proliferation and increases apoptosis in 22Rv1 cells[65] and the receptor is also abundantly expressed in PC-3 cells.[66]

Aspects in the design of XIAP inhibitors and mechanisms of action

It has previously been shown that cell death induced by IAP antagonism is absolutely dependent on TNFα and most cell lines that are sensitive to this treatment express elevated levels of TNFα or can be induced to produce TNFα upon treatment with IAP inhibitors.[17] This means that even if the caspases are relieved from the inhibition by XIAP, the cancer cells can still be unable to undergo apoptosis due to insufficient production of TNFα by the tumor. Since TNFα binds to the death receptor, diminished production of this cytokine could give less apoptosis initiated by the extrinsic pathway. To overcome this resistance, the XIAP inhibitory therapy can be combined with exogenously added TNFα.

To date six small molecular inhibitors of XIAP have entered clinical trials and they are all inspired by the tetra peptide (AVPI) IAP binding motif of the endogenous IAP inhibitor Smac.[9] As mentioned, this peptide binds preferentially to the BIR3 domain of XIAP, which targets initiator caspase 9 and thereby the intrinsic apoptotic pathway. However, it is the dimeric smac that can bind concurrently to the BIR3 and BIR2 domain of XIAP and thereby relive the inhibition of both caspase 9 and the downstream effector caspases 3 and 7, which efficiently relives inhibition of both apoptotic pathways (Fig. 3 and 4). Like the AVPI peptide shows higher affinity for the BIR3 domain so do the designed XIAP inhibitors since they are optimized for this interaction, but two of them are so called bivalent smac mimetic and can just like smac bind to both domains concurrently (in a step wise manner). The bivalent smac mimetic are much more potent in reliving caspase inhibition but due to their size they are not as suitable as drug candidates and need intravenous infusion and sometimes carrier peptides to be delivered into the cell, whereas the monovalent IAP inhibitors can be given orally.[9]

The small molecular XIAP inhibitors are active as single agents, meaning that cells do undergo apoptosis upon the treatment with these compounds without the addition of any apoptotic inducer (*e.g.* DR antibodies, Fas ligand, TRAIL, etoposide etc.). One paper argued that this was the case because caspases are already activated in cancer cells resembling the caspase status in *drosophila melanogaster*, but in contrast to normal mammalian cells.[67] A more precise explanation for this has been elucidated and it is now clear that these XIAP inhibitors just like smac rather are pan IAP inhibitors and preferentially inhibit the BIR3 domain of XIAP as well as the BIR3 domain of the ML-IAP, cIAP1 and cIAP2 members of the IAP family.[9, 68] The binding of a pan IAP inhibitor to cIAP BIR3 causes a conformational change leading to dimerization and increased E3 ligase activity of the RING domain.[69] This leads to ubiquitination of a protein called RIP1 and activation of the so-called canonical NF-κB pathway. Simultaneously, cIAP gets auto ubiquitinated and targets itself for proteosomal degradation. Once degraded, cIAP can no longer

function as a negative regulator of NIK (NF-κB-inducing kinase) and thereby also the non-canonical NF-κB pathway is activated.[68, 70]The activation of NF-κB leads to increased production of TNFα. This pro-inflammatory cytokine normally exerts more anti- than pro-apoptotic activity upon binding to TNF1R, but in the absence of cIAP, RIP1 remains unubiquitinated and can dissociate from the receptor complex and instead activate the initiator caspase 8 leading to apoptosis through the extrinsic pathway.[70]

In other words, the broad activity of today's pan IAP inhibitors leads initially to increased activity of cIAP as a positive regulator of the canonical NF-κB pathway and then, once degraded, cIAP can no longer negatively regulate the non-canonical NF-κB pathway leading to activation of that pathway as well. The intense activation of NF-κB leads to increased production of pro-inflammatory cytokines *e.g.* TNFα, which in absence of cIAP leads to initiation of the extrinsic apoptotic pathway through activation of caspase 8 and explains why the compounds are active as single agents but seem to depend on TNFα signaling. But since these inhibitors directly relive inhibition of caspase 9, increased levels of active caspase 9 are also achieved. Even when apoptotic pathways are blocked due to deficiencies in *e.g.* caspase 8, pan IAP inhibitors can cause cell death through TNFα mediated induction of necroptosis, which is another type of programmed cell death that in contrast does not depend on caspases.[71]

Like XIAP, cIAP1 is also overexpressed in most tumor tissues[17] and the broad activity of today's XIAP inhibitors is therefore desirable in the treatment of many cancers. In addition, these compounds work synergistically with many conventional chemotherapeutics as well as radiotherapy.[9] However, in B- and T-cells the activation of NF-κB leads to increased proliferation[72] and therefore the pan IAP inhibitors might not be suitable for treating lymphomas. Furthermore, the treatment with pan IAP inhibitors increases osteoclast activity and the risk of developing bone metastases in mice. If this is transferable to humans is not clear yet, but if it is, this could be potentially be mitigated with the administration of bisphosphonates.[73] Since the molecules synthesized in this project are inspired by embelin that targets the BIR3 domain of XIAP competitively with smac, it is possible that they exert anti-apoptotic effects through binding to XIAP as well as to cIAPs and ML-IAP, the latter possess anti-apoptotic activity through binding to and antagonizing smac.[9]

The simultaneous relief of inhibition of caspase 9 and caspase 3 and 7, but without consequent induction of NF-κB signaling pathways can be troublesome. One way to more selectively target XIAP is by designing molecules that targets the BIR2 domain of XIAP, or even better, the linker region between BIR1 and BIR2. The linker region binds the active caspases 3 and 7, whereas the BIR2 domain binds partially processed caspase 3 and 7. Even if some promiscuity to the BIR2 domain of cIAP1 might be hard to avoid when targeting XIAP BIR2, this will not induce NF-κB signaling.

In general, the BIR3 domain shows much higher preferences than the BIR2 domain when screening for tetra peptides capable of displacing AVPI peptides binding to BIR domains. However, the existence of an aromatic ring where the isoleucine in the AVPI peptide normally is positioned (as all smac mimetic and small molecular inhibitors of XIAP with published crystal structures possess) is not compatible with the Lys206 in BIR2. Instead this position (*i.e.* P4) in BIR2 prefer valine, alanine, glycine or isoleucine,[74] but since the AVPI motif with isoleucine in the P4 position rather binds to BIR3, mimicking valine, alanine or glycine might be preferred when selectively targeting BIR2.

Conclusion

The natural products embelin and nakijiquinone share a common quinone motif and bind to the in cancer frequently overexpressed proteins XIAP and IGF1R, respectively. Alkylated analogues of non-quinone fragments that mimic the physiochemical properties of embelin and nakijiquinone, and that in addition possess dual binding to XIAP and IGF1R, were synthesized. In order to prepare the alkylated analogues, conditions for Claisen rearrangement of allylated and fluoro-substituted salicylic acids were developed. The compounds were then evaluated in MTT proliferation assay for their potency of depleting viability in PC-3 and 22Rv1 prostate cancer cells.

Out of 25 tested molecules (fragments and their propylated analogues) one (**7**) was significantly more potent than the others and showed the same level of inhibition of proliferation as the propyl analogue of embelin in the castration resistant PC-3 cells. Even more strikingly, in the androgen dependent 22Rv1 cells, **7** exerted depletion of proliferation more potently than the propyl analogue of embelin (**41**) with viabilities of 11 % of untreated control for **7** compared with 37 % for **41** being measured at 400 μM.

Hopefully, an optimized variant of **7** will pioneer for a new type of cancer therapy that restores the apoptosis machinery by simultaneously acting on multiple targets. In the treatment of tumors that are capable of producing TNFα, the compound could be used as a single agent, but also in combination with well-tried cytotoxic agents or in combination with irradiation therapy. This approach could also give the patient a better chance to overcome resistance towards many of the anticancer therapies existing today. However, caution should be used when given together with chemotherapeutics with known neurotoxicity as both XIAP and IGF also protects neurons from apoptosis, [27, 10]and since IAP inhibitors activate osteoclasts,[73] more intense screening for bone metastases and treatment with antiresorptives might be beneficial.

Experimental procedures

General procedures

Unless otherwise stated, the reactions were performed in an inert atmosphere, with dry solvents, and the NMR spectra were recorded at 400 MHz (^{1}H) respective 100 MHz (^{13}C) on a Bruker spectrometer at 298 K, calibrated using the residual peak as internal standard: $CDCl_3$ ($CHCl_3$ δH 7.26 ppm, $CDCl_3$ δC 77.16 ppm), MeOH-d4 (CD_2HOD δH 3.31 ppm, CD_3OD δC 49.0 ppm). LC-MS was performed on a Micromass ZQ mass spectrometer with ES+ ionization. TLC was performed using Silica Gel 60 F254 and UV light detection and flash column chromatography was performed with normal phase silica gel (60 Å, 230-400 mesh, Merck, grade 9385). The reactions heated with microwave irradiation were performed on a Biotage, Initiator microwave oven.

5-Fluoro-2-hydroxy-benzoic acid benzyl ester (4)

5-Fluoro-2-hydroxy-benzoic acid (316 mg, 2.02 mmol), BnBr (360 μL, 3.03 mmol) and $KHCO_3$ (243 mg, 2.43 mmol) were dissolved in DMF (3 mL). After one day at room temperature, the reaction was monitored with TLC and diluted with EtOAc. Water was added and the organic layer was washed with 5

% aqueous $NaHCO_3$, and then with 5 % aqueous NaCl. The organic layer was dried over anhydrous Na_2SO_4 (s), filtered and concentrated *in vacuo*. The residue was then purified with flash chromatography (SiO_2, Heptane/EtOAc 97:3) to give a yield of 454 mg of **4** (91 %) as a clear liquid (crystalline in refrigerator). ^{1}H NMR ($CDCl_3$) δ: 10.56 (s, 1H), 7.56 (dd, 1H, J = 8.8, 3.2 Hz), 7.50-7.36 (m, 5H), 7.20 (ddd, 1H, J = 9.1, 7.9, 3.2 Hz), 6.96 (dd, 1H, J = 9.1, 4.5 Hz), 5.40 (s, 2H). ^{13}C NMR ($CDCl_3$) δ: 169.2 (d, J = 2.9 Hz), 158.1 (d, J = 1.5 Hz), 155.2 (d, J = 238.4 Hz), 135.1, 128.9 (2C), 128.8, 128.5 (2C), 123.4 (d, J = 24.2 Hz), 119.0 (d, J = 7.3 Hz), 115.2 (d, J = 24.2 Hz), 112.4 (d, J = 7.3 Hz), 67.4.

2-Allyloxy-5-fluoro-benzoic acid benzyl ester (5)

4 (89 mg, 0.36 mmol), allyl iodide (52 µL, 0.56 mmol), and Cs_2CO_3 (273 mg, 0.84 mmol) were dissolved in DMF (0.5 mL). The vial was flushed with argon and sealed. After two days at room temperature the reaction was diluted with water and extracted with diethyl ether. The organic layer was washed with 5 % aqueous $Na_2S_2O_3$, with saturated aqueous $NaHCO_3$, and finally with brine. The organic layer was dried over anhydrous Na_2SO_4 (s), filtered and concentrated *in vacuo*. The residue was then purified with flash chromatography (SiO_2, Heptane 100 % →Heptane/EtOAc 9:1) to give a yield of 96 mg of **5** (94 %) as a clear liquid. ^{1}H NMR ($CDCl_3$) δ: 7.56 (dd, 1H, J = 8.7, 3.3 Hz), 7.49-7.45 (m, 2H), 7.42-7.32 (m, 3H), 7.14 (ddd, 1H, J = 9.1, 7.5, 3.3 Hz), 6.91 (dd, 1H, J = 9.1, 4.3 Hz), 6.08-5.97 (m, 1H), 5.45 (dq, 1H, J = 17.2, 1.6 Hz), 5.37 (2H, s), 5.28 (dq, 1H, J = 10.5, 1.5 Hz), 4.57 (dt, 2H, J = 5.1, 1.5 Hz).^{13}C NMR ($CDCl_3$) δ: 164.9 (d, J = 2.2 Hz), 156.3 (d, J = 240.0 Hz), 154.6 (d, J = 2.2 Hz), 135.9, 132.7, 128.6 (2C), 128.29 (2C), 128.26, 121.5 (d, J= 6.6 Hz), 120.0 (d, J= 23.3 Hz), 118.2 (d, J= 24.9 Hz), 117.8, 115.4 (d, J= 8.1 Hz), 70.4, 66.9.

3-Allyl-5-fluoro-2-hydroxy-benzoic acid benzyl ester (6)

5 (50 mg, 0.17 mmol) was dissolved in NMP (2 mL) and heated at 200°C using microwave irradiation for 6 hours. The reaction was then diluted with water and extracted with diethyl ether. The organic layer was dried over anhydrous Na_2SO_4 (s), filtered and concentrated *in vacuo*. The residue was then purified with flash chromatography (SiO_2, 100 % Heptane → Heptane/EtOAc 95:5) to give a yield of 36 mg of **6** (72 %) as white crystals. ^{1}H NMR ($CDCl_3$) δ: 10.83 (s, 1H), 7.47-7.35 (m, 6H), 7.10 (dd, 1H, J = 8.8, 3.2 Hz), 6.04-5.91 (m, 1H), 5.38 (s, 2H), 5.15-5.13 (m, 1H), 5.12-5.08 (m, 1H), 3.42 (bd, 2H, J = 6.7 Hz). ^{13}C NMR ($CDCl_3$) δ: 169.7 (d, J = 2.9 Hz), 156.2 (d, J = 1.5 Hz), 154.9 (d, J = 237.7 Hz), 135.4, 135.2, 130.9 (d, J = 6.6 Hz), 128.9 (2C), 128.8, 128.5 (2C), 123.4 (d, J = 24.2 Hz), 116.9, 113.0 (d, J = 23.5 Hz), 111.9 (d, J = 8.1 Hz), 67.5, 33.7.

5-Fluoro-2-hydroxy-3-propyl-benzoic acid (7)

6 (13 mg, 0.045 mmol) and Pd/C (15 mg, 0.014 mmol, 10 wt. % Pd) were dissolved in MeOH (0.9 mL), the solution was then evacuated and purged with H_2 several times. Under a balloon of hydrogen and with vigorous stirring, the reaction was left overnight at room temperature. The reaction was monitored with LC-MS, diluted with MeOH, filtered through Celite, and then concentrated *in vacuo*. The residue was purified with flash chromatography (SiO_2, Heptane/EtOAc 4:1, HOAc 1 %) to give a yield of 9 mg of **7** (98 %) as a white powder. ^{1}H NMR (MeOD) δ: 7.36 (dd, 1H, J = 8.8, 3.2 Hz), 7.12 (dd, 1H, J = 9.0, 3.2 Hz), 2.64-2.59 (m, 2H), 1.70-1.57 (m, 2H), 0.96 (t, 3H, J = 7.4 Hz). ^{13}C NMR (MeOD) δ: 171.8 (d, J =2.9 Hz), 156.3 (d, J = 1.5 Hz), 154.5 (d, J = 236.1 Hz), 132.7 (d, J = 7.3 Hz), 122.3 (d, J = 23.5 Hz), 112.2 (d, J = 23.5 Hz), 112.0 (d, J = 7.3 Hz), 31.2 (d, J = 1.5 Hz), 22.1, 12.8.

5-Fluoro-2-propoxy-benzoic acid (8)

5 (36 mg, 0.12 mmol) and Pd/C (16 mg, 0.015 mmol, 10 wt. % Pd) were dissolved in MeOH (1.5 mL), the solution was then evacuated and purged with H_2 several times. Under a balloon of hydrogen and with vigorous stirring, the reaction was left for 3 hours at room temperature. The reaction was monitored with LC-MS, diluted with MeOH, filtered through Celite, and then concentrated *in vacuo*. The residue was purified with flash chromatography (SiO_2, Heptane/EtOAc 4:1, HOAc 1 %) to give a yield of 23 mg of **8** (94 %) as a white powder. ^{1}H NMR (MeOD) δ: 7.48 (dd, 1H, J = 8.9, 3.3 Hz), 7.24 (ddd, 1H, J = 9.1, 7.8, 3.3 Hz), 7.10 (dd, 1H, J = 9.2, 4.3 Hz), 4.03 (t, 2H, J = 6.4 Hz), 1.88-1.77 (m, 2H), 1.05 (t, 3H, J = 7.4 Hz). ^{13}C NMR (MeOD) δ: 168.5, 157.6 (d, 238.5 Hz), 156.1 (d, J = 2.2 Hz), 123.0 (d, J = 5.9 Hz), 121.0 (d, J = 22.8 Hz), 118.5 (d, J = 24.9 Hz), 116.3 (d, J = 8.0 Hz), 72.5, 23.5, 10.8.

4-Fluoro-2-hydroxy-benzoic acid benzyl ester (10)

4-Fluoro-2-hydroxy-benzoic acid (350 mg, 2.24 mmol), BnBr (467 µL, 3.92 mmol) and $KHCO_3$ (285 mg, 2.85 mmol) were dissolved in DMF (3 mL). After one day at room temperature, the reaction was monitored with TLC and diluted with EtOAc. Water was added and the organic layer was washed with 5 % aqueous $NaHCO_3$, and then with 5 % aqueous NaCl. The organic layer was dried over anhydrous Na_2SO_4 (s), filtered and concentrated *in vacuo*. The residue was then purified with flash chromatography (SiO_2, 100 % Heptane → Heptane/EtOAc 97:3) to give a yield of 497 mg of **10** (90 %) as a clear liquid. ^{1}H NMR ($CDCl_3$) δ: 11.09 (d, 1H, J = 1.5 Hz), 7.91 (dd, 1H, J = 8.8, 6.6 Hz), 7.51-7.38 (m, 5H), 6.72 (dd, 1H, J = 10.3, 2.5 Hz), 6.61 (ddd, 1H, J = 8.8, 8.5, 2.5 Hz), 5.41 (s, 2H). ^{13}C NMR ($CDCl_3$) δ: 169.4, 167.4 (d, J = 254.9 Hz), 163.9 (d, J = 13.9 Hz), 135.2, 132.2 (d, J = 11.0 Hz), 128.8 (2C), 128.7, 128.4 (2C), 109.2 (d, J = 2.9 Hz), 107.4 (d, J = 22.7 Hz), 104.4 (d, J = 24.2 Hz), 67.1.

2-Allyloxy-4-fluoro-benzoic acid benzyl ester (11)

10 (94 mg, 0.38 mmol), allyl iodide (52 µL, 0.56 mmol), and Cs_2CO_3 (256 mg, 0.78 mmol) were dissolved in DMF (0.5 mL). The vial was flushed with argon, sealed and shaken. After two days at room temperature the reaction was diluted with water and extracted with diethyl ether. The organic layer was washed with 5 % aqueous $Na_2S_2O_3$, with saturated aqueous $NaHCO_3$, and finally with brine. The organic layer was dried over anhydrous Na_2SO_4 (s), filtered and concentrated *in vacuo*. The residue was then purified with flash chromatography (SiO_2, Heptane 100 % →Heptane/EtOAc 9:1) to give a yield of 103 mg of **11** (94 %) as a white-clear liquid (crystalline in refrigerator). ^{1}H NMR ($CDCl_3$) δ: 7.95-7.86 (m, 1H), 7.50-7.43 (m, 2H), 7.42-7.31 (m, 3H), 6.72-6.64 (m, 2H), 6.08-5.97 (m, 1H), 5.49 (dq, 1H, J = 17.3, 1.6 Hz), 5.35 (s, 2H), 5.30 (dq, 1H, J = 10.6, 1.5 Hz), 4.59 (dt, 2H, J = 5.0, 1.6 Hz). ^{13}C NMR ($CDCl_3$) δ: 166.0 (d, J = 252.5 Hz), 165.1, 160.3 (d, J = 11.0 Hz), 136.2, 134.1 (d, J = 11.0 Hz), 132.1, 118.2, 116.4 (d, J = 2.9 Hz), 107.4 (d, J = 22.0 Hz), 101.4 (d, J = 25.7 Hz), 69.8, 66.7.

3-Allyl-4-fluoro-2-hydroxy-benzoic acid benzyl ester (12)

11 (50 mg, 0.17 mmol) was dissolved in NMP (2 mL) and run in micro oven at 200°C for 8 hours. The reaction was then diluted with water and extracted with diethyl ether. The organic layer was dried over anhydrous Na_2SO_4 (s), filtered and concentrated *in vacuo*. The residue was then purified with flash chromatography (SiO_2, 100 % Heptane → Heptane/EtOAc 95:5) to give a yield of 33 mg of **12** (66 %) as white crystals in a 9:1 mixture with the para Claisen rearranged isomer. Major product: ^{1}H NMR ($CDCl_3$)

δ: 11.28 (d, 1H, J = 2.0 Hz), 7.79 (dd, 1H, J = 8.9, 6.6 Hz), 7.49-7.34 (m, 5H), 6.60 (t, 1H, J = 8.9 Hz), 6.03-5.87 (m, 1H), 5.38 (s, 2H), 5.10-5.00 (m, 2H), 3.48-3.42 (m, 2H). ^{13}C NMR ($CDCl_3$) δ: 169.9, 165.4 (d, J = 253.1 Hz), 161.9 (d, J = 11.0 Hz), 135.36, 134.9, 129.6 (d, J = 11.9 Hz), 128.9 (2C), 128.73, 128.45 (2C), 115.55, 115.54 (d, J = 19.1 Hz), 108.8 (d, J = 2.6 Hz), 107.1 (d, J = 24.2 Hz), 67.2, 26.6 (d, J = 3.3 z).

4-Fluoro-2-propoxy-benzoic acid (13)

11 (58 mg, 0.20 mmol) and Pd/C (35 mg, 0.033 mmol, 10 wt. % Pd) were dissolved in MeOH (2.5 mL), the solution was then evacuated and purged with H_2 several times. Under a balloon of hydrogen and with vigorous stirring, the reaction was left for 3 hours at room temperature. The reaction was monitored with LC-MS, diluted with MeOH, filtered through Celite, and then concentrated *in vacuo*. The residue was purified with flash chromatography (SiO_2, Heptane/EtOAc 4:1, HOAc 1 %) to give a yield of 34 mg of **13** (83 %) as a white powder. ^{1}H NMR (MeOD) δ: 7.86 (dd, 1H, J = 8.7, 6.9 Hz), 6.87 (dd, 1H, J = 11.3, 2.3 Hz), 6.72 (ddd, 1H, J = 8.7, 8.0, 2.3 Hz), 4.03 (t, 2H, J = 6.3 Hz), 1.90-1.78 (m, 2H), 1.06 (t, 3H, J = 7.3 Hz). ^{13}C NMR (MeOD) δ: 168.8, 167.5 (d, J = 251.5 Hz), 162.0 (d, J = 11.0 Hz), 135.0 (d, J = 11.0 Hz), 117.7 (d, J = 2.9 Hz), 107.9 (d, J = 22.0 Hz), 102.0 (d, J = 26.4 Hz), 72.0, 23.3, 10.8.

4-Fluoro-2-hydroxy-3-propyl-benzoic acid (14)

12 (32 mg, 0.11 mmol) and Pd/C (22 mg, 0.021 mmol, 10 wt. % Pd) were dissolved in MeOH (1.5 mL), the solution was then evacuated and purged with H_2 several times. Under a balloon of hydrogen and with vigorous stirring, the reaction was left for 3 hours at room temperature. The reaction was monitored with LC-MS, diluted with MeOH, filtered through Celite, and then concentrated *in vacuo*. The residue was purified with flash chromatography (SiO_2, Heptane/EtOAc 4:1, HOAc 1 %) to give a yield of 9 mg of **14** (82 %) as a white powder in a 9:1 mixture with the para-claisen rearrangement product. Major product: ^{1}H NMR (MeOD) δ: 7.75 (dd, 1H, J = 9.0, 6.6 Hz), 6.60 (t, 1H, J = 9.0 Hz), 2.67-2.61 (m, 2H), 1.59 (sex, 2H, J = 7.4 Hz), 0.94 (t, 3H, J = 7.4 Hz). ^{13}C NMR (MeOD) δ: 173.4, 166.5 (d, J = 249.4 Hz), 163.4 (d, J = 11.0 Hz), 130.6 (d, J = 11.9 Hz), 118.4 (d, J = 19.1 Hz), 110.1 (d, J = 2.2 Hz), 107.3 (d, J = 24.3 Hz), 25.1 (d, J = 2.9 Hz), 23.2, 14.2.

5-Bromo-4-fluoro-2-hydroxy-benzoic acid (16)

NBS (269 mg, 1.51 mmol) was added to 4-Fluoro-2-hydroxy-benzoic acid (209 mg, 1.34 mmol) dissolved in DMF (2.7 mL) while stirring. The vial was covered with aluminum foil, flushed with argon, sealed and left at room temperature for two days. The reaction was then diluted with EtOAc and washed with water and brine several times. The organic layer was concentrated *in vacuo* and the residue was then dissolved in 0.1 M aqueous NaOH. 1 M aqueous HCl was added to the solution until the compound precipitated. The vial was then put on ice a few minutes before centrifugation at high speed for 5 minutes. The pellet was saved, while the supernatant (pink) was concentrated and subjected to the same work up procedure again. The pellets were then further purified with flash chromatography (SiO_2, Heptane/EtOAc 1:2, HOAc 1.5 %) to give a yield of 194 mg of **16** (62%) as a white powder. ^{1}H NMR (MeOD) δ: 8.06 (d, 1H, J = 8.1 Hz), 6.80 (d, 1H, J = 10.1 Hz). ^{13}C NMR (MeOD) δ: 171.74, 164.4 (d, J = 12.9 Hz), 164.3 (d, J = 253.1 Hz), 136.2 (d, J = 3.1 Hz), 112.4 (d, J = 2.9 Hz), 106.2 (d, J = 24.9 Hz), 98.8 (d, J = 22.4 Hz).

5-Bromo-4-fluoro-2-hydroxy-benzoic acid benzyl ester (17)

BnBr (114 µL, 0.96 mmol) and $KHCO_3$ (71 mg, 0.71 mmol) were added to **16** (129 mg, 0.55 mmol) dissolved in DMF (1.5 mL). The vial was flushed with argon, sealed and run at room temperature for two days. After TLC monitoring the reaction was diluted with EtOAc, washed with water, 5 % aqueous $NaHCO_3$, 5 % aqueous NaCl, water, and brine respectively. The organic layer was dried over anhydrous Na_2SO_4 (s), filtered and concentrated *in vacuo*. The residue was then purified with flash chromatography (SiO_2, Heptane/EtOAc 95:5→ 9:1) to give a yield of 175 mg of **17** (98 %). ^{1}H NMR ($CDCl_3$) δ: 10.95 (d, 1H, J = 1.6 Hz), 8.06 (d, 1H, J = 7.8 Hz), 7.52-7.34 (m, 5H), 6.77 (d, 1H, J = 9.0 Hz), 5.39 (s, 2H). ^{13}C NMR ($CDCl_3$) δ: 168.5, 163.3 (d, J = 255.2 Hz), 162.9 (d, J = 12.9 Hz), 134.9, 134.7 (d, J = 3.2 Hz), 129.2-128.3 (m, 5C), 67.7.

2-Allyloxy-5-bromo-4-fluoro-benzoic acid benzyl ester (18)

Allyl iodide (49 µL, 0.54 mmol) and Cs_2CO_3 (232 mg, 0.71 mmol) were added to **17** (110 mg, 0.34 mmol) dissolved in DMF. The vial was flushed with argon, sealed and shaken. After two days at room temperature the reaction was diluted with water and extracted with diethyl ether. The organic layer was washed with 5 % aqueous $Na_2S_2O_3$, with saturated aqueous $NaHCO_3$, and finally with brine. The organic layer was dried over anhydrous Na_2SO_4 (s), filtered and concentrated *in vacuo*. The residue was then purified with flash chromatography (SiO_2, Heptane/EtOAc 95:5 → 87:13) to give a yield of 103 mg of **18** (83 %) as a liquid. ^{1}H NMR ($CDCl_3$) δ: 8.07 (d, 1H, J = 8.1 Hz), 7.48-7.32 (m, 5H), 6.75 (d, 1H, J = 10.4 Hz), 6.08-5.93 (m, 1H), 5.47 (dq, 1H, J = 17.2, 1.5 Hz), 5.33 (s, 2H), 5.31 (dq, 1H, J = 10.6, 1.4 Hz), 4.58 (dt, 2H, J = 5.0, 1.5 Hz). ^{13}C NMR ($CDCl_3$) δ: 164.0, 162.0 (d, J = 253.9 Hz), 159.4 (d, J = 9.5 Hz), 136.7 (d, J = 2.9 Hz), 135.9, 131.7, 128.7 (2C), 128.4 (3C), 118.6, 117.9 (d, J = 3.6 Hz), 102.7 (d, J = 26.4 Hz), 99.2 (d, J = 21.3 Hz), 70.2, 67.1.

3-Bromo-4-fluoro-2-hydroxy-5-propenyl-benzoic acid (21)

$Pd(OAc)_2$ (4 mg, 0.016 mmol), *cis*-Propenylboronic acid (35 mg, 0.41 mmol), and Na_2CO_3 (63 mg, 0.59 mmol) were added to **20** (54 mg, 0.17 mmol) dissolved in H_2O (1.5 mL). The reaction was run for three days at room temperature and was then diluted with water and filtered through Celite with water and then with diethyl ether. The filtrate was acidified with 10 % aqueous HCl and extracted several times with diethyl ether. The combined organic layers were then dried over anhydrous Na_2SO_4 (s), filtered and concentrated *in vacuo*. The residue was then subjected to flash chromatography (SiO_2, Heptane/EtOAc 9:1, HOAc 2 %→ 8:2, HOAc 2 %) and gave a yield of 11 mg of **21** (24 %) as a white powder. ^{1}H NMR (MeOD) δ: 7.86 (bd, 1H, J = 8.3 Hz), 6.33 (bd, 1H, J = 11.5 Hz), 5.97-5.88 (m, 1H), 1.82-1.78 (m, 3H).

2-Allylamino-4-fluoro-benzoic acid (23)

Allyl alcohol (307 µL, 4.51 mmol) and $Pd(PPh_3)_4$ (119 mg, 0.10 mmol) were added to 2-Amino-4-fluoro-benzoic acid (233 mg, 1.50 mmol) dissolved in THF/H_2O (1:1, 5 mL). The reaction vial was purged with argon and sealed. After three days at room temperature the reaction was diluted with water and extracted with EtOAc. The combined organic layers were dried over anhydrous Na_2SO_4 (s), filtered and concentrated *in vacuo*. The residue was then subjected to flash chromatography (SiO_2, Heptane/EtOAc 9:1, 1 % HOAc→ 3:2, 1 % HOAc) and gave a yield of 281 mg of **23** (96 %) as a white-beige powder. ^{1}H NMR ($CDCl_3$) δ: 8.01-7.95 (m, 1H), 6.37-6.29 (m, 2H), 5.98-5.88 (m, 1H), 5.30 (dq, 1H, J = 17.2, 1.3 Hz),

5.23 (dq, 1H, J = 10.4, 1.3 Hz), 3.87 (dt, 2H, J = 5.0, 1.6 Hz). ^{13}C NMR ($CDCl_3$) δ: 173.7, 168.1 (d, J = 252.9 Hz), 153.9 (d, J = 13.2 Hz), 135.5 (d, J = 12.1 Hz), 133.8, 116.7, 105.6 (d, J = 1.5 Hz), 103.2 (d, J = 23.5 Hz), 98.1 (d, J = 25.7 Hz), 45.4.

4-Fluoro-2-propylamino-benzoic acid (24)

23 (20 mg, 0.10 mmol) and Pd/C (10 mg, 0.0094 mmol, 10 wt. % Pd) were dissolved in MeOH (1.5 mL), the solution was then evacuated and purged with H_2 several times. Under a balloon of hydrogen and with vigorous stirring, the reaction was left overnight at room temperature. The reaction was monitored with LC-MS, diluted with MeOH, filtered through a syringe filter, and concentrated *in vacuo*. The residue was then subjected to flash chromatography (100 % Heptane, 2 % HOAc→ Heptane/EtOAc 8:2, 2 % HOAc) to give a yield of 11 mg of **24** (54 %) as a white powder. ^{1}H NMR (MeOD) δ: 7.90 (dd, 1H, J = 8.6, 7.1 Hz), 6.38 (dd, 1H, J = 12.4, 2.2 Hz), 6.25 (dt, 1H, J = 8.6, 2.2 Hz), 3.13 (bs, 2H), 1.68 (sex, 2H, J = 7.3 Hz), 1.03 (t, 3H, J = 7.3 Hz). ^{13}C NMR (MeOD) δ: 171.0, 168.7 (d, J = 249.5 Hz), 155.0, 136.1 (d, J = 11.0 Hz), 108.2, 102.5 (d, J = 22.8 Hz), 98.0 (d, J = 24.9 Hz), 45.5, 23.3, 11.9.

2-Allylamino-4-fluoro-benzoic acid benzyl ester (25)

$KHCO_3$ (56 mg, 0.56 mmol) and **23** (73 mg, 0.37 mmol) were dissolved in DMF (2 mL) and left to stir at room temperature for one hour. BnBr (47 µL, 0.39 mmol) was added to the reaction and the vial was purged with argon and sealed. After 40 hours at room temperature and LC-MS monitoring, the reaction was diluted with EtOAc and washed several times with water. The organic layer was dried over anhydrous Na_2SO_4 (s), filtered and concentrated *in vacuo*. The residue was then subjected to flash chromatography (SiO_2, Heptane/EtOAc 98:2→ 95:5, 5 % HOAc) and gave a yield of 99 mg of **25** (93 %) as a clear liquid. ^{1}H NMR ($CDCl_3$) δ: 8.07 (bs, 1H), 8.00 (dd, 1H, J = 8.9, 6.9 Hz), 7.46-7.32 (m, 5H), 6.35-6.25 (m, 2H), 5.98-5.87 (m, 1H), 5.31 (s, 2H), 5.30 (dq, 1H, J = 17.2, 1.5 Hz), 5.21 (dq, 1H, J = 10.3, 1.5 Hz), 3.87-3.81 (m, 2H). ^{13}C NMR ($CDCl_3$) δ: 167.8, 167.4 (d, J = 251.2 Hz), 153.4 (d, J = 12.5 Hz), 136.4, 134.4 (d, J = 11.7 Hz), 134.0, 128.7 (2C), 128.3, 128.1 (2C), 116.6, 106.8 (splitted), 102.7 (d, J = 22.8 Hz), 97.9 (d, J = 26.4 Hz), 66.2, 45.5.

2-Allylamino-5-fluoro-benzoic acid (28)

Allyl alcohol (53 µL, 0.78 mmol) and $Pd(PPh_3)_4$ (13 mg, 0.011 mmol) were added to 2-Amino-5-fluoro-benzoic acid (40 mg, 0.26 mmol) dissolved in THF/H_2O (1:1, 0.5 mL). The reaction vial was purged with argon and sealed. After three days at room temperature the reaction was diluted with water and extracted with EtOAc. The combined organic layers were dried over anhydrous Na_2SO_4 (s), filtered and concentrated *in vacuo*. The residue was then subjected to flash chromatography (SiO_2, Heptane/EtOAc 9:1, 2 % HOAc) and gave a yield of 47 mg of **28** (94 %) as a yellow powder. ^{1}H NMR ($CDCl_3$) δ: 7.67 (dd, 1H, J = 9.6, 3.2 Hz), 7.16 (ddd, 1H, J = 9.3, 7.7, 3.2 Hz), 6.62 (dd, 1H, J = 9.3, 4.4 Hz), 5.99-5.89 (m, 1H), 5.29 (dq, 1H, J = 17.2, 1.5 Hz), 5.21 (dq, 1H, J = 10.4, 1.5 Hz), 3.89 (dt, 2H, J = 5.0, 1.7 Hz). ^{13}C NMR ($CDCl_3$) δ: 173.3 (splitted), 153.1 (d, J = 233.9 Hz), 148.7, 134.4, 123.7 (d, J = 23.4 Hz), 117.5 (d, J = 23.2 Hz), 116.5, 113.2 (d, J = 7.0 Hz), 108.6 (d, J = 6.6 hz), 45.7.

5-Fluoro-2-propylamino-benzoic acid (30)

28 (20 mg, 0.10 mmol) and Pd/C (10 mg, 0.0094 mmol, 10 wt. % Pd) were dissolved in MeOH (1.5 mL), the solution was then evacuated and purged with H_2 several times. Under a balloon of hydrogen and with vigorous stirring, the reaction was left overnight at room temperature. The reaction was monitored with LC-MS, diluted with MeOH, filtered through a syringe filter, and concentrated *in vacuo*. The residue was then subjected to flash chromatography (100 % Heptane, 2 % HOAc→ Heptane/EtOAc 8:2, 2 % HOAc) to give a yield of 12 mg of **30** (57 %) as a yellow powder. ^{1}H NMR (MeOD) δ: 7.54 (dd, 1H, J = 9.8, 3.2 Hz), 7.13 (ddd, 1H, J = 9.2, 8.0, 3.2 Hz), 6.70 (dd, 1H, J = 9.2, 4.4 Hz), 3.14 (t, 2H, J = 6.9 Hz), 1.67 (sex, 2H, J = 7.3 Hz), 1.02 (t, 3H, J = 7.3 Hz). ^{13}C NMR (MeOD) δ: 171.0 (d, J = 2.5 Hz), 154.2 (d, J = 231.6 Hz), 149.6, 122.9 (d, J = 23.4 Hz), 117.9 (d, J = 23.1 Hz), 113.6 (d, J = 7.0 Hz), 111.3 (d, J = 6.3 Hz), 45.9, 23.4, 11.9.

1-Allyl-4-trifluoromethyl-1H-pyrimidin-2-one (33)

SPhos (7 mg, 0.018 mmol), $[PdCl(C_3H_5)]_2$ (3 mg, 0.0085 mmol), KF (44 mg, 0.76 mmol), and **32** (20 mg, 0.082 mmol) were dissolved in a 9:1 mixture of dioxane/H_2O (0.8 mL). Allylboronic acid pinacol ester (60 µL, 0.33 mmol) was added and the vial was sealed, shaken and flushed with argon. The reaction was run in micro oven for 20 min at 110°C and then monitored with LC-MS. The reaction is diluted with EtOAc and washed with H_2O. The aqueous layer is extracted with EtOAc and the combined organic layers were dried over anhydrous Na_2SO_4 (s), filtered and concentrated *in vacuo*. The residue was purified with flash chromatography (SiO_2, CH_2Cl_2/EtOAc 10:1) and gave a yield of 6 mg of **33** (33 %). ^{1}H NMR ($CDCl_3$) δ: 7.90 (d, 1H, J = 6.8 Hz), 6.60 (d, 1H, J = 6.8 Hz), 6.05-5.92 (m, 1H), 5.48-5.29 (m, 2H), 4.60 (bd, 2H, J = 6.2 Hz).

1-Benzyl-5-bromo-4-trifluoromethyl-1H-pyrimidin-2-one (35)

32 (20 mg, 0.082 mmol) was dissolved together with Cs_2CO_3 (38 mg, 0.12 mmol) in DMF (0.8 mL). BnBr (12 µL, 0.099 mmol) was added and the reaction was run for 20 hours at room temperature. Then the reaction was monitored by TLC, diluted with EtOAc, and washed several times with water before wash with brine. The organic layer was dried over anhydrous Na_2SO_4 (s), filtered and concentrated *in vacuo*. The residue was purified with flash chromatography (SiO_2, Heptane/EtOAc 2:1) and gave a yield of 7 mg of **35** (26 %). ^{1}H NMR ($CDCl_3$) δ: 7.87 (s, 1H), 7.48-7.35 (m, 5H), 5.13 (s, 2H).

2-Benzyloxy-4-trifluoromethyl-pyrimidine (38)

2-Chloro-4-trifluoromethyl-pyrimidine (50 mg, 0.27 mmol), CuI (5 mg, 0.027 mmol), 1.10-Phenanthroline (10 mg, 0.055 mmol) and Cs_2CO_3 (134 mg, 0.41 mmol) were dissolved in toluene (345 µL). BnOH (284 µL, 1.00 mmol) was added and the vial was flushed with argon and sealed. After two days at 120°C, the reaction is diluted with EtOAc and filtered through a plug of silica. Then concentrated *in vacuo* and purified with flash chromatography (SiO_2, Heptane/EtOAc 8:1) to give a yield of 45 mg of **38** (65 %) as white crystals. ^{1}H NMR (360 MHz, $CDCl_3$) δ: 8.77 (d, 1H, J = 4.9 Hz), 7.54-7.48 (m, 2H), 7.41-7.30 (m, 3H), 7.26 (d, 1H, J = 4.9 Hz), 5.50 (s, 2H).

Biological experiments

To be mentioned, there were no ethical considerations when performing the experiments.

Cell lines and cultures

The androgen-independent human prostate cancer cell line PC-3 and the androgen-dependent cell line 22Rv1 (American Type Culture Collection) were grown in RPMI 1640 (Invitrogen, Stockholm, Sweden) with 10 % fetal bovine serum (FBS; Invitrogen) and gentamycin (50 µg/mL, Invitrogen) at 37°C, in a humified atmosphere with 5 % CO_2. This culture media were used in all experiments when seeding the cells.

Cell viability assay

Cells were seeded in culture medium (described above) on 96-well plates with 0.1 mL media/well. The 22Rv1 cells were seeded with 20 000 cells/well and the PC-3 cells were seeded with 5000 cells/well. The number of viable cells was determined by using a Countess™ automated cell counter (Invitrogen) with cells diluted 1:1 in 0.4 % trypan blue. Twenty-four hours after seeding the medium was changed to phenol- and FBS free α-mem (Invitrogen) and after an additional 24 hours of incubation the cells were subjected to the synthesized molecules at different concentrations (as indicated in figure 9, 10, and 11). The molecules were dissolved in DMSO to a final concentration of 0.5 % in fresh α-mem media. The cells were then left to respond to the molecules during 72 hours, without changing the media.
The viability of the cells was then analyzed with Cell Proliferation Kit I (Roche Diagnostics, Bromma, Sweden) according to manufacturer's instruction, by measuring the conversion of 3(4,5-dimethythiazozyl-2)-2,5 diphenyl tetrazolium bromide (MTT) into purple formazan. MTT is a tetrazolium salt that can be reduced into purple formazan by intracellular NADP(H) dependent reductases. The NADPH concentration is higher in metabolically active cells and therefor more formazan is formed in living cells than in dead cells. The concentration of formazan is after solubilization measured by UV-spectrometry ($\lambda^{1\text{-}2}$, 590-650 nm) and thereby gives an indication of the amount of living cells.

Acknowledgements

Thanks to Sofie Knutsson and Andreas Larsson (Department of Chemistry, Umeå University), Luciana Auzzas (Istituto di Chimica Biomolecolare, CNR, Sassari, Italy), Annika Nordstrand (Department of Oncology, Umeå University), and Pernilla Wikström (Department of Pathology, Umeå University) for guidance throughout this project.

References

1. Zimmermann GR, Lehár J, Keith CT (2007). Multi-target therapeutics: when the whole is greater than the sum of the parts. Drug Discov. Today. 12, 34–42.

2. Hanahan D, Weinberg RA (2000). The Hallmarks of Cancer. Cell 100, 57–70.

3. McKenzie S, Kyprianou N (2006). Apoptosis Evasion: The Role of Survival Pathways in Prostate Cancer Progression and Therapeutic Resistance. J. Cell Biochem. 97, 18–32.

4. McCarty MF (2004). Targeting multiple signaling pathways as a strategy for managing prostate cancer: Multifocal signal modulation therapy. Integr. Cancer Ther. 3, 349–380.

5. Taylor RC, Cullen SP, Martin SJ (2008). Apoptosis: Controlled demolition at the cellular level. Nat. Rev. Mol. Cell. Biol. 9, 231–241.

6. Chang HY, Yang X (2000). Proteases for cell suicide: functions and regulation of caspases. Microbiol. Mol. Biol. Rev. 64, 821-846.

7. Lin YF *et al.* (2013). Targeting the XIAP/caspase-7 complex selectively kills caspase-3–deficient malignancies. J Clin Invest. 123, 3861–3875.

8. Teague SJ, Davis AM, Leeson PD, and Oprea TI (1999). The design of leadlike combinatorial libraries. Angew. Chem., Int. Ed. Engl. 38, 3743.

9. Fulda S, Vucic D (2012). Targeting IAP proteins for therapeutic intervention in cancer. Nat. Rev. Drug Discov. 11, 109-124.

10. Haisa M (2013). The type 1 insulin-like growth factor receptor signalling system and targeted tyrosine kinase inhibition in cancer. J. Int. Med. Res. 41, 253-264

11. Valentinis B, Baserga R (2001). IGF-I receptor signalling in transformation and differentiation. Mol Pathol. 54, 133–137.

12. Suzuki Y, Nakabayashi Y, Takahashi R (2001). Ubiquitin-protein ligase activity of X-linked inhibitor of apoptosis protein promotes proteosomal degradation of caspase-3 and enhances its anti-apoptotic effect in Fas-induced cell death. Proc. Natl. Acad. Sci. USA 98, 8662–8667.

13. Nikolovska-Coleska Z *et al.* (2004). Discovery of embelin as a cell-permeable, small-molecular weight inhibitor of XIAP through structure-based computational screening of a traditional herbal medicine three-dimensional structure database. J. Med. Chem. 47, 2430-2440.

14. Stahl P, Kissau L, Mazitschek R, Giannis A, Waldmann H (2002). Natural product derived receptor tyrosine kinase inhibitors: Identification of IGF1R, Tie-2, and VEGFR-3 Inhibitors. Angew. Chem. Int. Ed. Engl. 41, 1174–1178.

15. Kaighn ME, Narayan KS, Ohnuki Y, Lechner JF, Jones LW (1979). Establishment and characterization of a human prostatic carcinoma cell line (PC-3). Invest. Urol. 17, 16-23.

16. Sramkoski RM *et al.* (1999). A new human prostate carcinoma cell line, 22Rv1. In Vitro Cell Dev. Biol. Anim. 35, 403-409.

17. de Almagro MC, Vucic D (2012). The inhibitor of apoptosis (IAP) proteins are critical regulators of signaling pathways and targets for anti-cancer therapy. Exp. Oncol. 34, 200-211.

18. Crook NE, Clem RJ, Miller LK (1993). An apoptosis-inhibiting baculovirus gene with a zinc finger-like motif. J. Virol. 67, 2168-2174.

19. Liston P, Fong WG, Korneluk RG (2003). The inhibitors of apoptosis: there is more to life than Bcl2. Oncogene. 22, 8568-8580.

20. Eckelman BP, Salvesen GS, Scott FL (2006). Human inhibitor of apoptosis proteins: why XIAP is the black sheep of the family. EMBO Rep. 7, 988-994.

21. Ashkenazi A (2008). Targeting the extrinsic apoptosis pathway in cancer. Cytokine Growth F. R. 19, 325-331.

22. Özören N, El-Deiry WS (2002). Defining Characteristics of Types I and II Apoptotic Cells in Response to TRAIL. Neoplasia. 4, 551–557.

23. Fulda S, Galluzzi L, Kroemer G (2010). Targeting mitochondria for cancer therapy. Nat. Rev. Drug Discov. 9, 447-464.

24. Owens TW, Foster FM, Valentijn A, Gilmore AP, Streuli CH (2010). Role for X-linked Inhibitor of apoptosis protein upstream of mitochondrial permeabilization. J. Biol. Chem. 285, 1081-1088.

25. Huang Y, Rich RL, Myszka DG, Wu H (2003). Requirement of Both the Second and Third BIR Domains for the Relief of X-linked Inhibitor of Apoptosis Protein (XIAP)-mediated Caspase Inhibition by Smac. J. Biol. Chem. 278, 49517-49522.

26. Sun H, Nikolovska-Coleska Z , Yang ZY, Qian D, Lu J, Qiu S, Bai L, Peng Y, Cai Q, Wang S (2008). Design of Small-Molecule Peptidic and Nonpeptidic Smac Mimetics. Acc. Chem. Res. 41, 1264–1277.

27. LaCasse EC (2013). Pulling the plug on a cancer cell by eliminating XIAP with AEG35156. Cancer Lett. 332, 215–224.

28. Dohi T *et al.* (2004). An IAP-IAP Complex Inhibits Apoptosis. J. Biol. Chem. 279, 34087–34090.

29. Fukuda S, Pelus LM (2006). Survivin, a cancer target with an emerging role in normal adult tissues. Mol. Cancer Ther. 5, 1087-1098.

30. Mehrotra S, Languino LR, Raskett CM, Mercurio AM, Dohi T, Altieri DC (2010). IAPregulation of metastasis. Cancer Cell. 17, 53-64.

31. Gyrd-Hansen M, Meier P (2010). IAPs: from caspase inhibitors to modulators of NF-kappaB, inflammation and cancer. Nat. Rev. Cancer. 10, 561-574.

32. Wu ZH, Wong ET, Shi Y, Niu J, Chen Z, Miyamoto S, Tergaonkar V (2010). ATM- and NEMO-dependent ELKS ubiquitination coordinates TAK1-mediated IKK activation in response to genotoxic stress. Mol. Cell. 40, 75-86.

33. Zha J, Lackner MR (2010). Targeting the insulin-like growth factor receptor-1R pathway for cancer therapy. Clin. Cancer Res. 16, 2512-2517.

34. Massagué J, Czech MP (1982). The subunit structures of two distinct receptors for insulin-like growth factors I and II and their relationship to the insulin receptor. J. Biol. Chem. 257, 5038-5045.

35. Chen YW, Boyartchuk V, Lewis BC (2009). Differential roles of insulin-like growth factor receptor- and insulin receptor-mediated signaling in the phenotypes of hepatocellular carcinoma cells. Neoplasia. 11, 835-845.

36. Thorner MO, Strasburger CJ, Wu Z, Straume M, Bidlingmaier M, Pezzoli SS, Zib K, Scarlett JC, Bennett WF (1999). Growth hormone (GH) receptor blockade with a PEG-modified GH (B2036-PEG) lowers serum insulin-like growth factor-I but does not acutely stimulate serum GH. J. Clin. Endocrinol. Metab. 84, 2098-2103.

37. Shelton JG, Steelman LS, White ER, McCubrey JA (2004). Synergy between PI3K/Akt and Raf/MEK/ERK pathways in IGF-1R mediated cell cycle progression and prevention of apoptosis in hematopoietic cells. Cell Cycle. 3, 372-379.

38. Tognon CE, Sorensen PH (2012). Targeting the insulin-like growth factor 1 receptor (IGF1R) signaling pathway for cancer therapy. Expert. Opin. Ther. Targets. 16, 33-48.

39. Sarbassov DD, Guertin DA, Ali SM, Sabatini DM (2005). Phosphorylation and regulation of Akt/PKB by the rictor-mTOR complex. Science. 307, 1098-1101.

40. Braulke T (1999). Type-2 IGF receptor: a multi-ligand binding protein. Horm. Metab. Res. 31, 242-246.

41. Martin-Kleiner I, Gall Troselj K (2010). Mannose-6-phosphate/insulin-like growth factor 2 receptor (M6P/IGF2R) in carcinogenesis. Cancer Lett. 289, 11-22.

42. Munshi S, Hall DL, Kornienko M, Darke PL, Kuo LC (2003). Structure of apo, unactivated insulin-like growth factor-1 receptor kinase at 1.5 A resolution. Acta. Crystallogr. D. 59, 1725-1730.

43. Kasuya J, Paz IB, Maddux BA, Goldfine ID, Hefta SA, Fujita-Yamaguchi Y (1993). Characterization of human placental insulin-like growth factor-I/insulin hybrid receptors by protein microsequencing and purification. Biochemistry 32, 13531–13536.

44. Pandini G, Vigneri R, Costantino A, Frasca F, Ippolito A, Fujita-Yamaguchi Y, Siddle K, Goldfine ID, Belfiore A (1999). Insulin and insulin-like growth factor-I (IGF-I) receptor overexpression in breast cancers leads to insulin/IGF-I hybrid receptor overexpression: evidence for a second mechanism of IGF-I signaling. Clin. Cancer Res. 5, 1935-1944.

45. Pandini G, Frasca F, Mineo R, Sciacca L, Vigneri R, Belfiore A (2002). Insulin/insulin-like growth factor I hybrid receptors have different biological characteristics depending on the insulin receptor isoform involved. J. Biol. Chem. 277, 39684-39695.

46. Hubbard RD, Wilsbacher JL (2007). Advances towards the development of ATP-competitive small-molecule inhibitors of the insulin-like growth factor receptor (IGF-IR). Chem. Med. Chem. 2, 41-46.

47. Bohula EA, Playford MP, Macaulay VM (2003). Targeting the type 1 insulin-like growth factor receptor as anti-cancer treatment. Anticancer Drugs. 14, 669-682.

48. Arteaga CL, Kitten LJ, Coronado EB, Jacobs S, Kull FC Jr, Allred DC, Osborne CK (1989). Blockade of the type I somatomedin receptor inhibits growth of human breast cancer cells in athymic mice. J. Clin. Invest. 84, 1418-1423.

49. Goya M *et al.* (2004). Growth inhibition of human prostate cancer cells in human adult bone implanted into nonobese diabetic/severe combined immunodeficient mice by a ligand-specific antibody to human insulin-like growth factors. Cancer Res. 64, 6252-6258.

50. D'Ambrosio C, Ferber A, Resnicoff M, Baserga R (1996). A soluble insulin-like growth factor I receptor that induces apoptosis of tumor cells in vivo and inhibits tumorigenesis. Cancer Res. 56, 4013-4020.

51. Lee JS, Weiss J, Martin JL, Scott CD (2003). Increased expression of the mannose 6-phosphate/insulin-like growth factor-II receptor in breast cancer cells alters tumorigenic properties in vitro and in vivo. Int. J. Cancer. 107, 564–570.

52. Zhang X, Yee D (2002). Insulin-like growth factor binding protein-1 (IGFBP-1) inhibits breast cancer cell motility. Cancer Res. 62, 4369-4375.

53. Claisen, L (1912). Über Umlagerung von Phenol-allyläthern inC-Allyl-phenole. Ber. Dtsch. Chem. Ges. 45, 3157–3166.

54. Guo W, Li J, Fan N, Wu W, Zhou P, Xi C (2005). A simple and effective method for chemoselective esterification of phenolic acids. Synthetic Commun. 35, 145-152.

55. Dong Fang S *et al*. (2011). Preparation of benzofuran derivatives as GPR120 receptor agonists. U.S. Pat. Appl. Publ., 0313003.

56. Bumagin NA, Bykov VV (1997). Ligandless palladium catalyzed reactions of arylboronic acids and sodium tetraphenylborate with aryl halides in aqueous media.Tetrahedron. 53, 14437-14450.

57. Hikawa H, Yokoyama Y (2011). Palladium-catalyzed mono-N-allylation of unprotected anthranilic acids with allylic alcohols in aqueous media. J. Org. Chem. 76, 8433–8439.

58. Majumdar KC, Bhattacharyya T, Chattopadhyay B, Sinha B (2009). Recent advances in the aza-Claisen rearrangement. Synthesis. 13, 2117-2142.

59. Anderson WK, Gaifa L (1995). Boron trifluoride-diethyl ether complex catalyzed aromatic amino-Claisen rearrangements. Synthesis. 10, 1287-1290.

60. Ondi L, Lefebvre O, Schlosser M (2004). Brominated 4-(Trifluoromethyl)pyrimidines: A convenient access to versatile intermediates. Eur JOC. 3714-3718.

61. Zanatta N *et al*. (2008). Comparative study of the chemoselectivity and yields of the synthesis of N Alkyl4-(trihalomethyl)-1 H -pyrimidin-2-ones. Eur JOC. 5832-5838.

62. Nara SJ, Jha M, Brinkhorst J, Zemanek TJ, Pratt DA (2008). A simple Cu-catalyzed coupling approach to substituted 3-pyridinol and 5-pyrimidinol antioxidants. J. Org. Chem. 73, 9326–9333.

63. Mosmann T (1983). Rapid colorimetric assay for cellular growth and survival: Application to proliferation and cytotoxicity assays. J. Immunol. Methods 65, 55–63.

64. Danquah M, Duke CB 3rd, Patil R, Miller DD, Mahato RI (2012). Combination therapy of antiandrogen and XIAP inhibitor for treating advanced prostate cancer. Pharm Res. 29, 2079-2091.

65. Konijeti R *et al*. (2012). Effect of a low-fat diet combined with IGF-1 receptor blockade on 22Rv1 prostate cancer xenografts. Mol. Cancer Ther. 11, 1539–1546.

66. Khandwala HM, McCutcheon IE, Flyvbjerg A, Friend KE (2000). The effects of insulin-like growth factors on tumorigenesis and neoplastic growth. Endocr. Rev. 21, 215–244.

67. Huang Y, Lu M, Wu H (2004). Antagonizing XIAP-mediated caspase-3 inhibition. Achilles' heel of cancers? Cancer Cell. 5, 1-2.

68. Vince JE *et al.* (2007). IAP antagonists target cIAP1 to induce TNFalpha-dependent apoptosis. Cell. 131, 682-693.

69. Feltham R *et al.* (2011). Smac mimetics activate the E3 ligase activity of cIAP1 protein by promoting RING domain dimerization. J. Biol. Chem. 286, 17015-17028.

70. Varfolomeev E *et al.* (2007). IAP antagonists induce autoubiquitination of c-IAPs, NF-kappaB activation, and TNFalpha-dependent apoptosis. Cell. 131, 669-681.

71. Laukens B *et al.* (2011). Smac mimetic bypasses apoptosis resistance in FADD- or caspase-8-deficient cells by priming for tumor necrosis factor α-induced necroptosis. Neoplasia. 13, 971-979.

72. Lim KH, Yang Y, Staudt LM (2012). Pathogenetic importance and therapeutic implications of NF-κB in lymphoid malignancies. Immunol. Rev. 246, 359-378.

73. Yang C *et al.* (2013). Antagonism of inhibitor of apoptosis proteins increases bone metastasis via unexpected osteoclast activation. Cancer Discov. 3, 212-223.

74. Lukacs C *et al.* (2013). The structure of XIAP BIR2: understanding the selectivity of the BIR domains. Acta Cryst. D. 69, 1717-1725.

75. Li J, Mercer E, Gou X, Lu YJ (2013). Ethnical disparities of prostate cancer predisposition: genetic polymorphisms in androgen-related genes. Am. J. Cancer Res. 3, 127-151.

Department of Chemistry
S-901 87 Umeå, Sweden
Telephone +46 90 786 50 00
Text telephone +46 90 786 59 00
www.umu.se